



የኢ.ፌ.ዲ.ሪ የቴክኒክና ሙያ  
ስልጠና አንስቲቲዩት  
FDRE TECHNICAL & VOCATIONAL  
TRAINING INSTITUTE

**TECHNICAL AND VOCATIONAL TRAINING  
INSTITUTE (TVTI)**

**School of Graduate Studies**

**FACULTY OF ELECTRICAL AND ELECTRONICS  
TECHNOLOGY AND INFORMATION AND COMMUNICATION  
TECHNOLOGY  
DEPARTMENT OF ELECTRICAL AND ELECTRONICS  
TECHNOLOGY**

**ENERGY EFFICIENCY OPTIMIZATION TECHNIQUES FOR 5G  
ULTRA DENSE WIRELESS NETWORKS USING MASSIVE MIMO**

A Thesis Proposal for the Partial Fulfillment of  
Masters of Science (MSc) in Electronics & communication Technology Management

*By,*

**ZINABU NEGASH (TTMR/243/16)**

*Supervisor,*

**Anand Anbalagan (PhD)**

*March 2026*

*Addis Ababa, Ethiopia*



የኢ.ፌ.ዲ.ሪ የቴክኒክና ሙያ  
ስልጠና አንስተኞች  
FDRE TECHNICAL & VOCATIONAL  
TRAINING INSTITUTE

**ENERGY EFFICIENCY OPTIMIZATION TECHNIQUES FOR 5G ULTRA  
DENSE WIRELESS NETWORKS USING MASSIVE MIMO**

*A Thesis proposal submitted to*  
**TECHNICAL AND VOCATIONAL TRAINING INSTITUTE (TVTI)**

**FACULTY OF ELECTRICAL AND ELECTRONICS TECHNOLOGY AND  
INFORMATION AND COMMUNICATION TECHNOLOGY  
(DEPARTMENT OF ELECTRICAL AND ELECTRONICS TECHNOLOGY)**

*In partial fulfillment for the Degree*  
**MASTERS OF SCIENCE in ELECTRONICS AND COMMUNICATION TECHNOLOGY  
MANAGEMENT**

*By,*  
**Zinabu Negash (TTMR/243/16)**

*Supervisor,*  
**Anand Anbalagan (PhD)**

## ***DECLARATIONS***

I hereby declare that the work which is being presented in this thesis proposal, entitled Energy Efficiency Optimization Techniques for 5G Ultra-Dense Wireless Networks Using Massive MIMO, is the original work of my own, has not been presented for a degree in this or other universities, and all sources of materials used for this thesis work have been fully acknowledged.

Name: Zinabu Negash (TTMR/243/16)



Signature: -----

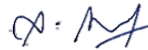
Place: Addis Ababa

Date of Submission: -----

This thesis proposal has been submitted for examination with my approval as a TVTI advisor.

Anand Anbalagan (PHD)

Advisor Name



Signature-----

Date-----


**TECHNICAL AND VOCATIONAL TRAINING INSTITUTE (TVTI)  
FACULTY OF ELECTRICAL AND ELECTRONICS TECHNOLOGY AND  
INFORMATION AND COMMUNICATION TECHNOLOGY  
(DEPARTMENT OF ELECTRICAL AND ELECTRONICS TECHNOLOGY)**

*Thesis Proposal on*

**ENERGY EFFICIENCY OPTIMIZATION TECHNIQUES FOR 5G ULTRA  
DENSE WIRELESS NETWORKS USING MASSIVE MIMO**

By,  
**ZINABU NEGASH (TTMR/243/16)**

APPROVED BY THESIS ADVISORY COMMITTEE

Name of the Advisor	Signature	Date
<u>Anand Anbalagan(PhD)</u>	 -----	-----
Name of the Examiner, Internal	Signature	Date
-----	-----	-----
Name of the Examiner, External	Signature	Date
-----	-----	-----
Name of the Chairperson	Signature	Date
-----	-----	-----

## **Acknowledgment**

I sincerely thank Almighty God for granting me strength, wisdom, and guidance throughout this journey. I extend my deepest gratitude to my advisor, Dr. Anand Anbalgan, for his invaluable guidance, motivation, constructive feedback, and continuous support, which were essential to the successful completion of this thesis.

I also express my appreciation to my family for their unwavering support, and to the department of Electrical and Electronics Communication Technology and my friends for their encouragement and assistance in completing this research.

## ABSTRACT

With the fast development of wireless communication systems, lowering energy utilization in these systems has resulted in an essential requirement for network operators. In the context of 5G wireless networks, the concept of energy efficiency (EE) has been recognized as an important performance measure. Optimizing the network design will result in considerable savings in terms of total power consumption, especially with the incorporation of massive MIMO (multiple input multiple output) technology.

This study is concentrated on optimizing the efficiency of 5G ultra-dense wireless networks with massive MIMO architecture. The optimization is carried out on three important factors, namely, pre-coding strategies, channel state information, Dinkel Bach fraction programming, and the massive MIMO system architecture. A comprehensive model is developed for circuit power consumption, incorporating the time division duplex protocol, zero-forcing pre-coding, and maximizing the efficiency of the system. The Dinkel Bach fraction programming is also incorporated in the optimization process, where the maximum EE is obtained by maximizing the EE function.

The system parameters are also studied in detail, namely, the number of base station antennas, the number of active users, system throughput, and network density. The concept of energy efficiency is also discussed, where the total number of bits transmitted is divided by the total power consumption in the system. The MATLAB programming environment is used to simulate the system, where the relationship between these parameters and EE optimization is studied.

The results obtained show that the optimal configuration of M, K, and R will result in maximum energy efficiency in the system. The Dinkel Bach fraction programming is also seen to outperform the conventional zero-forcing pre-coding method, where the EE is maximized in the system.

**Keywords:** massive MIMO; energy efficiency; CSI; Dinkel Bach algorithm, 5G, ZF precoding

# Contents

ABSTRACT .....	II
Contents.....	III
List of figures .....	VI
List of tables.....	VII
List of abbreviations and acronyms .....	VIII
CHAPTER ONE .....	1
INTRODUCTION .....	1
1.1 Background .....	1
1.2 Objectives.....	3
1.2.1 General objective.....	3
1.2.2 Specific objectives.....	3
1.3 Statement of the problem .....	4
1.4 Scope of the thesis.....	4
1.5 Limitation.....	4
1.6 Significance of the study .....	5
1.7 Methodology .....	6
1.8. Organization of the Thesis .....	8
CHAPTER TWO .....	9
LITERATURE REVIEW .....	9
2.1 Related Works .....	9
2.2 Literature summary .....	11
2.3 Energy efficiency optimization techniques for 5g ultra-dense wireless networks.....	12
2.4 Transmission channel.....	12
2.5 Ultra-dense wireless communication .....	15
2.6 Multi-user MIMO.....	16
2.8 Massive Multiple Input Multiple Output System (Massive MIMO) .....	17
2.8.1 Features of Massive MIMO .....	19
2.8.2 Energy efficiency of Massive MIMO .....	20
2.8.3 Massive MIMO Channel Estimation.....	20
2.8.4 Massive MIMO Channel Model .....	21
2.8.5 Massive MIMO Data Transmission Protocol.....	22
2.8.6 Massive MIMO Uplink Data Transmission.....	22

2.8.7 Massive MIMO Downlink Data Transmission .....	23
2.8.8 Pre-coding techniques in massive MIMO.....	23
2.8.9 Linear pre-coding schemes in MIMO .....	24
2.9 Limitations of Massive MIMO .....	25
2.9.1 Pilot Contamination.....	25
2.9.2 Unfavorable Propagation.....	26
2.9.3 Energy efficiency techniques in 5G wireless communications.....	26
2.9.4 Massive MIMO Power Consumption .....	27
2.9.5 System Parameters in Massive MIMO.....	28
2.9.7 Uplink in Massive MIMO System .....	31
2.9.8 Downlink in Massive MIMO System .....	34
2.9.5 Massive MIMO Systems Existing Power Consumption Model .....	37
CHAPTER THREE .....	38
ENERGY EFFICIENCY OPTIMIZATION FOR 5G ULTRA DENSE WIRELESS COMMUNICATION NETWORKS USING MASSIVE MIMO SYSTEMS .....	38
3.1 System model .....	38
3.2 Evaluation of Total Power Consumption in Massive MIMO Systems.....	40
3.3 Massive MIMO Circuit-Level Power Consumption.....	40
3.3.3 Circuit Power for channel Coding and Decoding ( $P_{C/D}$ ) .....	41
3.3.4 Backhaul Circuit Power ( $P_{BH}$ ).....	42
3.3.5 Linear Processing Circuit Power ( $p_{LP}$ ) .....	42
3.4 Achievable Sum Rate .....	42
3.5 Maximizing Energy Efficiency in Massive MIMO Using ZF Processing.....	43
3.6 Energy Efficiency optimization with Dinkel Bach algorithm in Massive MIMO for 5G ultra-dense networks .....	45
3.5.1 Energy efficiency optimization and the influence of multiple active users .....	48
3.5.2 Energy efficiency optimization and the influence of multiple active antennas .....	49
3.5.3 Energy efficiency optimization and the influence of transmit power .....	50
3.5.4 Energy efficiency optimization and the influence of throughput.....	50
CHAPTER FOUR.....	51
SIMULATION AND RESULTS DISCUSSION .....	51
4.1 Introduction .....	51
4.2 Simulation parameters.....	51
4.3 Simulation and result discussion .....	52

4.3.1 Impact of the number of massive base station antennas on energy efficiency optimization .....	52
4.3. 2.Impact of the number of active users on energy efficiency optimization .....	54
4.3.4 Impact of transmit power on energy efficiency optimization. ....	57
4.3.5 The impact of cell density on energy efficiency optimization .....	58
4.3.6 The relationship between energy efficiency and spectra efficiency .....	60
4.3.7 The relationship between energy efficiency and data rate .....	61
4.3.8 Optimizing energy efficiency by using Massive MIMO .....	63
CHAPTER FIVE: .....	65
CONCLUSION AND RECOMMENDATIONS.....	65
5.1 Conclusion.....	65
5.2 Recommendations .....	66
References .....	67

## List of figures

Figure1 . follow the chart of the whole work.....	7
Figure 2.1 signal propagation in wireless channel.....	12
figure 2.2 mu-mimo .....	16
Figure 2.2 spatial multiplexing .....	17
Figure 2.3 Concepts of massive MIMO technology.....	19
Figure 2.4 TDD with coherence interval .....	22
Figure 2.5 massive mimo uplink.....	22
Figure 2.6 massive mimo down link.....	23
Figure 2.7 Pilot contamination in massive mimo .....	25
Figure 2.8 Unfavorable propagation in massive MIMO.....	26
Figure 2.9: Overview of Energy Efficiency Techniques in Wireless Communications.....	27
Figure 3.1 generic multiuser MIMO.....	29
Figure 3.1: Overall work follow chart .....	39
Figure 4.1 simulation of EEs antenna.....	52
Figure 4.2 Simulation of EEs user .....	54
Figure 4.3 Simulation of EEs throughput( varying k) .....	55
Figure 4.4 Simulation of EEs transmit power.....	57
Figure 4.5 Simulation of EEs cell density .....	58
Figure 4.6 EEs SE.....	60
Figure 4.7 EE VS data rate .....	61
Figure 4.8 3D simulation of EEs (K, M) .....	63

## List of tables

Table 1 summary of literature review .....	11
Table 2: Definition of Power Consumption Coefficient.....	44
Table 3 Simulation parameters .....	51
Table 4. Energy Efficiency (Mb/J) vs Number of Antennas .....	53
Table 5 Energy Efficiency (Mb/J) vs Number of Users .....	55
Table 6 Energy Efficiency (Mb/J) vs Throughput (Mbps) .....	56
Table 7 Energy Efficiency (Mb/J) vs Transmit Power per User (W) .....	58
Table8. Simulation result of EE vs cell density .....	60
Table.9 Simulation result of EE vs SE.....	61
Table. 10. EE VS data rate.....	62
Table 11 comparison our work with related previous work .....	64

## List of abbreviations and acronyms

3GPP	Third Generation Partnership Project
4G	Fourth Generations
5G	Fifth Generation
ADC	Analog-to-Digital Converter
AoA	Angle of Arrival
AP	Access Point
ASIC	Application-Specific Integrated Circuit
AWGN	Additive White Gaussian Noise
BBU	Baseband Unit
BS	Base Station
CBS	Cellular Base Station
CLT	Central Limit Theory
CP	Circuit Power
CSI	Channel State Information
DAC	Digital-to-Analog Converter
DC	Digital Converter
DL	Downlink
DPA	Downlink Packet Access
EE	Energy Efficiency
FDD	Frequency Division Duplexing
FIX	Fixed
GPP	Generation Partnership Project
GW	Gateway
HSDPA	High-Speed Downlink Packet Access
HSPA	High-Speed Packet Access

i.i.d	Independent and Identically Distributed
IEEE	Institute of Electrical and Electronics Engineers
ISI	Inter-Symbol Interference
ITU	International Telecommunication Union
LMMSE	Linear Minimum Mean Square Error
MIMO	Multiple-Input Multiple-Output
MMIMO	Massive Multiple-Input Multiple-Output
MMSE	Minimum Mean Square Error
MR	Maximum Ratio
MRC	Maximum Ratio Combining
MRT	Maximum Ratio Transmission
MU	Multi-User
OFDMA	Orthogonal Frequency Division Multiple Access
PA	Power Amplifier
PFIX	Fixed Power
PSM	Power Save Mode
RAT	Radio Access Technology
REC	Radio Equipment Control
SDMA	Space Division Multiple Access
SE	Spectral Efficiency
SIC	Successive Interference Cancellation
SINR	Signal-to-Interference-plus-Noise Ratio
SNR	Signal-to-Noise Ratio
TDD	Time Division Duplex
UDN	Ultra-Dense Network
UTRA	Universal Terrestrial Radio Access
ZF	Zero Forcing

# CHAPTER ONE

## INTRODUCTION

### 1.1 Background

The fast evolution of intelligent devices and their broad applications has led to a substantial growth in multimedia service requirements. The increase in transmission capacity of wireless networks has ensured that the quality of service (QoS) requirements of mobile applications are satisfied[1]. Meanwhile, telecommunication manufacturers and network operators have predicted that the traffic load of wireless communication networks is growing exponentially[2]. Recent industry reports indicate that global 5G adoption has accelerated rapidly, with billions of mobile subscriptions now supported by 5G networks worldwide, the majority of which are driven by smartphone users. At the same time, mobile data traffic continues to grow at an unprecedented rate, following a near-exponential trend. Video services, including high-definition streaming, immersive media, and real-time applications, account for the majority of traffic and place significant pressure on existing network infrastructure. Meanwhile, high power consumption in wireless networks increases carbon emissions and operational costs annually [3] [4]. Therefore, Energy Efficiency (EE) has emerged as a key metric for evaluating wireless communication system performance under practical constraints. Meanwhile, Multiple-Input Multiple-Output (MIMO) technology has gained significant attention due to its ability to substantially improve data throughput and link reliability without increasing bandwidth or transmit power[5].

The MIMO concept was proposed and patented in 1993–1994, introducing multiple transmit antennas at a single transmitter to enhance link throughput [6]. MIMO is a core technology in 5G systems, and when an eNB with multiple antennas serves multiple UEs on the same time frequency resources, it is known as MU-MIMO[7]. By leveraging multiplexing and diversity gains, MU-MIMO enhances system throughput or communication reliability [2]. Massive MIMO proposed by [8] Scaling up these demands is a crucial approach in wireless system design. Massive MIMO has demonstrated the ability to improve spectral efficiency and reduce transmit power, making it a crucial technology for next-generation systems to enhance both SE and EE[9] . Conventional MIMO is limited to controlling signal transmission only in the horizontal plane when the antenna array (AA) down-tilt is fixed. To exploit the vertical dimension, the 3rd Generation Partnership Project (3GPP) studied various AA structures, including rectangular, spherical, and cylindrical designs[10] 3D MIMO uses

these arrays to adjust azimuth and elevation angles, supporting 3D signal propagation. To boost capacity, more antennas are deployed for greater multiplexing gains, and practical Massive MIMO systems adopt rectangular, spherical, and cylindrical arrays considering array space[11]. Therefore, 3D MIMO with large-scale arrays enables practical Massive MIMO deployment, which boosts spectral efficiency through high multiplexing gains when serving multiple UEs simultaneously[12]. EE increases considerably as additional antennas focus energy on targeted UEs using highly directional beams. [13].With excessive degrees of freedom, Massive MIMO can achieve higher transmission reliability [5]. It reduces Inter-User Interference (IUI) due to its extremely narrow beam [1]. Likewise, it closely approaches the performance of optimal techniques, such as Zero Forcing (ZF)),[14], With Maximum-Likelihood multiuser detection and DPC, signal processing can be implemented using simple, low-complexity algorithms [15]. Optimization of Energy-Efficient Techniques for 5G ultra-dense wireless communication networks using massive MIMO is designed to advance coverage-tier base stations by utilizing antenna arrays with hundreds of elements, each operating at relatively low transmit power. The system enables coherent multiuser MIMO, allowing multiple users to simultaneously transmit and receive via spatial multiplexing in both uplink and downlink. Massive MIMO enhances area throughput by exploiting multiplexing gains to improve overall system performance[16]. The current study investigates methods to optimize energy efficiency through power management in 5G ultra-dense networks that employ massive MIMO technology. The research aims to optimize energy efficiency through power management of user equipment, which will result in energy output exceeding energy input. Energy Efficiency optimization methods will be used with Massive MIMO technology in 5G systems to implement zero forcing and Dinkel Bach algorithm.

## **1.2 Objectives**

### **1.2.1 General objective**

To optimize energy efficiency in 5G ultra-dense wireless networks using Massive MIMO techniques, considering throughput, antenna number, user density, and circuit power constraints.

### **1.2.2 Specific objectives**

- To apply and evaluate Dinkel Bach's algorithm with Zero-Forcing (ZF) precoding to optimize energy efficiency in 5G ultra-dense networks under perfect and imperfect CSI.
- To model and analyze the total circuit power consumption in Massive MIMO systems for defining and optimizing overall energy efficiency.
- To assess the influence of a large number of base station antennas on system energy efficiency.
- To analyze the effect of multiple active users on energy efficiency optimization.
- To examine the relationship between data throughput and energy efficiency in Dinkel Bach optimized scenarios.
- To simulate and evaluate the system under various design parameters using MATLAB.

### **1.3 Statement of the problem**

As wireless communication systems expand, the amount of energy they consume has become a pressing issue, particularly for network operators managing ultra-dense infrastructures. In recent years, base stations have consumed a substantial amount of power, resulting in tens of millions of tons of CO<sub>2</sub> emissions annually, and this figure continues to increase with the ongoing expansion of cellular networks. This trend contributes to higher operational costs and considerable environmental issues. In the era of 5G, improving energy efficiency is not optional. It is a core requirement. Existing network configurations suffer from suboptimal energy use, particularly as user demand and data rates increase. Therefore, there is a need for research that identifies energy-optimizing strategies without compromising Quality of Service (QoS), especially through optimal use of design parameters like antenna count, user density, and throughput.

### **1.4 Scope of the thesis**

This study focuses on optimizing energy efficiency of 5G wireless communication systems by utilizing Massive MIMO technology in ultra-dense network environments. The focus is limited to the analysis and simulation of circuit power consumption models and the evaluation of the influence of critical system parameters (number of antennas, users, and throughput) on energy efficiency. The study uses Dinkel Bach's algorithm and Zero Forcing (ZF) linear pre-coding under TDD communication protocols and simulates various CSI conditions using MATLAB.

### **1.5 Limitation**

- Hardware-specific power consumption metrics (e.g., RF front-end losses, power amplifier inefficiencies) are modeled theoretically and not measured experimentally.
- The study evaluates perfect and imperfect CSI but does not cover advanced channel estimation techniques in detail.
- Mobility and Doppler effects in high-speed user environments are not incorporated

## **1.6 Significance of the study**

This research provides valuable insights into designing energy-efficient 5G networks, particularly in scenarios involving ultra-dense deployments and Massive MIMO systems. By identifying optimal combinations of antennas, users, and throughput, the study contributes to the sustainable development of wireless infrastructures, reducing both operational costs and environmental impact.

The findings can help:

- Network engineers design systems with better energy-performance trade-offs.
- Telecommunication companies reduce power bills while meeting rising data demands. Academics and researchers further explore energy-efficient techniques in next-generation wireless technologies.

## 1.7 Methodology

The following approaches were used to address the mentioned problems

Literature review

- Comprehensive review of previous works on 5G, Massive MIMO, and energy efficiency techniques.
- Identifying existing challenges in energy consumption modeling and performance optimization.

Collecting data: The researchers collected secondary data sources on energy efficiency optimization, and mathematical models of energy optimization techniques were studied.

System Modeling: Development of a mathematical model for total power consumption.

- Circuit power components are broken down into:
  - Transceiver Circuit Power
  - Channel Estimation Circuit Power
  - Coding/Decoding Power
  - Backhaul Power

Simulation: The developed system was simulated using MATLAB

Results, Discussion, and Conclusions: Finally, the results, discussion, conclusions, and future work are presented.

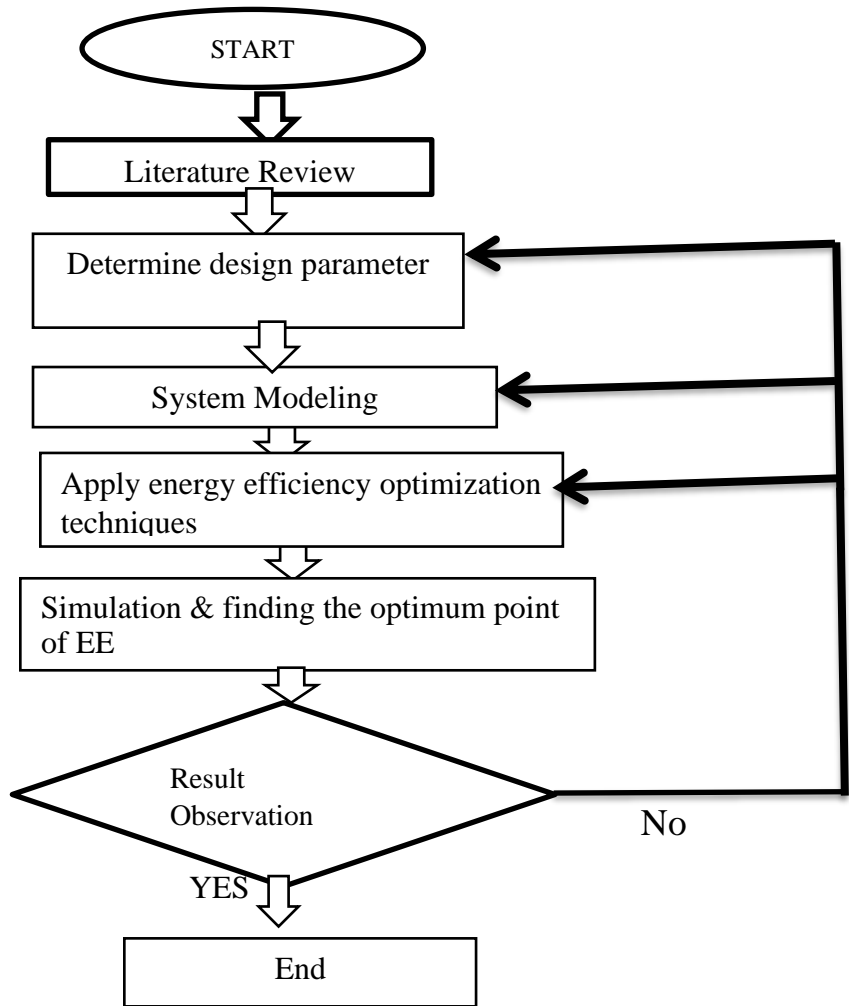


Figure1 . follow the chart of the whole work

## **1.8. Organization of the Thesis**

This research has five chapters that maintain an interconnection with each other. Complete Chapter reading is necessary for readers to understand the thesis contributions. The introduction of the first chapter presents the main research topic of the thesis through its literature review, objective, statement of problem, scope, significance of the study, and methodology explanation.

The second chapter of the study presents the fundamental concepts that explain energy efficiency techniques used in 5G wireless networks while demonstrating how massive MIMO and dense technology improve energy efficiency assessment.

The third chapter of the system model presents energy efficiency optimization techniques used in 5G systems through an explanation of research topics and background information, which includes system models and formulas, and existing theories and techniques used to optimize EE, which were used in this thesis research with corresponding justification details.

The fourth chapter presents the simulation procedures used in the research study. The study presents data which includes testing simulation results displayed in graphical form, together with results analysis.

The fifth chapter presents the implementation results through their implications and conclusion, together with a recommendation for future work.

## **CHAPTER TWO**

### **LITERATURE REVIEW**

#### **2.1 Related Works**

In contemporary wireless communication systems, energy efficiency (EE) has emerged as a vital metric for evaluating network performance, especially as the information and communication technology (ICT) sector continues to grow[17][18]. Numerous studies have explored methods to reduce energy consumption in 5G wireless networks, with particular focus on base stations (BSs), which are responsible for more than 60% of total network energy usage[19] [20].

An energy-aware, load-adaptive framework for dynamic antenna operation in base stations was proposed in [21]. The study explained EE of high, medium, and low traffic conditions, respectively, compared with conventional static systems. Similarly, Marwaha et al. [22].Extended this work by jointly optimizing the number of active antennas, physical resource block (PRB) scheduling, and spatial layering in heterogeneous networks (Het Nets). Their adaptive algorithm demonstrated significant EE improvements under varying load conditions.

Abu-Bakr et al.[22] Proposed a lightweight, threshold-based clustering and search algorithm for energy-efficient cell switching in ultra-dense Het Nets. The approach minimized power consumption while maintaining near-optimal network performance. Ngo et al. [23]Conducted a comprehensive survey on ultra-dense Cell-Free Massive MIMO (CF-MMIMO) systems for beyond-5G and 6G applications, identifying challenges such as front-haul constraints, synchronization, low-complexity processing, and resource allocation as critical issues in achieving optimal EE.

In [12] A semi-orthogonal hybrid RF-chain architecture was introduced to reduce radio frequency (RF) hardware complexity while maintaining both energy and spectral efficiency. This design effectively enhanced scalability by minimizing the hardware overhead of massive MIMO systems. Poi rot [1]investigated EE improvement strategies for low-traffic conditions using BS sleep modes and cell-breathing mechanisms. Although effective in reducing energy consumption, these techniques introduced latency issues due to BS reactivation delays, highlighting a trade-off between energy conservation and quality of service (QoS).

Yang [1] focused on optimizing the number of antennas per BS in multi-cell massive MIMO systems under power control constraints. Their findings revealed that employing identical antenna

configurations across BSs had minimal impact on overall EE due to the flat nature of the EE function. However, their analysis did not consider variations in user density or data rate. Similarly, Björnson and Sanguinetti [15][24] utilized stochastic geometry to optimize EE by adjusting BS density, antenna count, user numbers, transmit power, and pilot reuse factors. While comprehensive, their work did not address the influence of system throughput on QoS.

Desset and Debaillie [16][25] analyzed the power consumption of MIMO systems by examining various precoding schemes and refining digital processing power models. Although their study provided valuable insights into component-level energy usage, it did not assess how variations in antenna numbers and user equipment affect overall EE. Abbas and Adnan [25] Conducted a case study to determine the optimal number of antennas and users that maximize EE without degrading spectral efficiency. Their analysis, however, excluded circuit power consumption, which is essential for a complete EE evaluation. Isabona and Srivastava [18] investigated the trade-off between achievable sum rates and EE in downlink massive MIMO systems using linear and non-linear precoding techniques. Their findings indicated that non-linear successive interference cancellation (SIC) pre-coding enhances EE in micro and pico-cell networks, but the impact of the number of active users on total system EE was not considered.

## 2.2 Literature summary

Most of the studies mentioned above aim to enhance energy efficiency in wireless communication networks. However, they often overlook key variables or model simplifications that affect system-wide optimization.[26]. Notably, inconsistencies exist in modeling circuit power consumption and key design parameters such as antenna count, user density, and throughput. In contrast, the current thesis identifies and includes these often-omitted parameters, specifically circuit power and critical system variables (M, K, and R), to conduct a more complete evaluation of EE in massive MIMO-enabled 5G networks.

*Table 1 summary of literature review*

Authors	Study focus	Identified gaps
Liu, H.; Deng, H.; Yi, Y.; Zhu, Z.; Liu, G.; Zhang, J(2022)	Energy-efficient power allocation for massive MIMO downlink systems using optimization-based algorithms.	The analysis assumes perfect CSI at the base station, which is unrealistic in practical systems due to pilot contamination, estimation errors, and feedback delay.
Ibrahim Salah, M. Mourad Mabrook, Kamel Hussein (2022)	GA-based energy efficiency optimization for adaptive massive MIMO in 5G	Does not fully capture channel condition, backhaul, and cooling power consumption
Vahid Khodamoradi ,Aduwati Sali , Oussama messadi1, Asem a. salah, Mohanad m. al-wani , Borhanuddin mohd ali (2020)	Energy-efficient power adaptation for downlink multi-cell massive MIMO	Assumption of Perfect Channel State Information (CSI) only.
Al-Kamali et al. (2023)	□ Focuses heavily on mm Wave and line-of-sight (LoS)	LoS-only models; ideal phase shifters assumed
Tian et al. (2019)	focus is on spectral performance, with limited EE	High complexity; weak energy-efficiency analysis
Björnson & Sanguinetti (2019–2020)	EE optimization using stochastic geometry considering BS density, antennas, and users.	The impact of throughput and QoS constraints on EE was not explicitly analyzed

### 2.3 Energy efficiency optimization techniques for 5g ultra-dense wireless networks

Energy efficiency (EE) optimization in Ultra-dense 5G networks employing Massive MIMO technology. focuses on maximizing the amount of data transmitted per unit of energy while meeting QoS, coverage, and system constraints. Energy efficiency is measured as the amount of data transmitted per unit power (bits/J. Ultra-dense deployments enhance coverage and spectral efficiency, but they also increase energy consumption due to higher transmit power, circuit processing, and backhaul costs. Massive MIMO enhances EE via spatial multiplexing and beamforming, serving multiple users with lower per-user power, but adds circuit and processing overhead. Optimizing EE balances these gains against energy costs.

### 2.4 Transmission channel

The transmission channel serves as a medium through which electromagnetic waves propagate during wireless transmission. Because these waves are not confined to a single propagation path, they undergo reflection, diffraction, and scattering from buildings, terrain, human bodies, and other obstacles

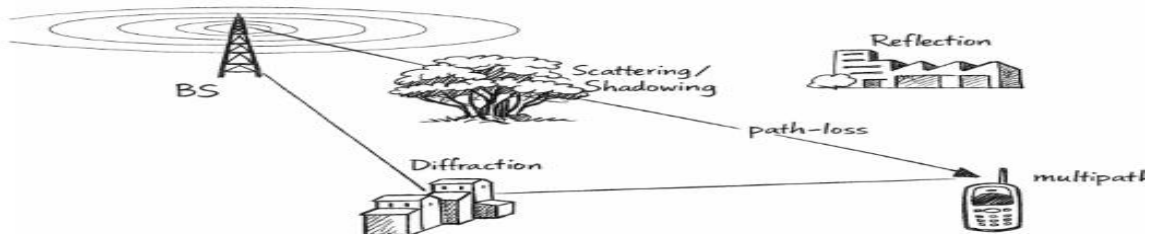


Figure 2.1 signal propagation in wireless channel

Wireless signals rarely travel directly; they reflect, scatter, or diffract around obstacles, reaching the receiver at different times and strengths. Their combination can strengthen (constructive) or weaken (destructive) the signal, a phenomenon called multipath propagation. The communication medium is primarily affected by Distance-dependent loss, shadow effects, and multipath fading [28]. The path loss in a vacuum or free space is expressed as

$$L = \frac{(4\pi d)^2}{G_t G_r \epsilon^2} \quad (2.1)$$

Here,  $\varepsilon$  is the wavelength,  $G_t$  and  $G_r$  are the transmitter and receiver antenna gains, and  $d$  is the distance between them. The model is valid only for direct line-of-sight with a single propagation path. In cellular communication, the signal travels through multiple transmission routes that connect the transmitter with the receiver, and path-loss is typically estimated using the following model.

$$L = \zeta d - \alpha \quad (2.2)$$

Here,  $\zeta$  represents antenna and channel effects, while  $\alpha$  is the path-loss exponent (typically 2–6). Shadowing is the random signal variation caused by obstacles through scattering, reflection, and diffraction [8]. The log-normal shadowing model is a widely used statistical method for modeling shadowing, where the random variable  $y$  follows a defined probability density function (PDF).

$$F_y = \frac{\mathbf{1}}{y\sigma\sqrt{2\pi}} e^{-\frac{\ln y - \mu}{(2\alpha)^2}} \quad (2.3)$$

$\mu$  and  $\sigma$  denote the mean and standard deviation of  $y$  in dB, respectively.

Small-scale fading denotes the minuscule differences in the channel caused by the superposition of the multi-path signal replicas through constructive and destructive interference. Each replica, in an ultra-dense 5G wireless system with a massive MIMO setup, the signal gets to experience different kinds of attenuations, delays, and phase shifts while being conveyed through the wireless medium. The combination of all the signal components can boost the received signal (constructive addition) or reduce it (destructive addition) [24].

A signal in extreme weakening is in a deep fade. Fading can be analyzed via coherence bandwidth  $W_c$ , the frequency range over which the channel is highly correlated. If the signal bandwidth is less than  $W_c$ , the channel appears uniform, causing flat fading. Coherence bandwidth decreases with larger delay spread from multipath, making the channel more frequency-selective.

$$W_c = \frac{\mathbf{1}}{Td} \quad (2.4)$$

Here,  $Td$  is the difference between the earliest and latest significant multipath delays. If the signal bandwidth is smaller than the channel's coherence bandwidth, the channel shows flat fading. When it exceeds the coherence bandwidth, the channel becomes frequency-selective, causing distortion and inter-symbol interference (ISI). Equalization can mitigate this but adds complexity, so modern

systems use multi-carrier schemes like OFDM, dividing the signal into narrow subcarriers that each experience flat fading, reducing ISI [17].

The time-domain variation of fading is characterized by the coherence time  $T_c$ , defined as the duration over which the channel response remains highly correlated. It is inversely related to the Doppler spread  $f_d$ , which quantifies the rate of channel variation caused by relative motion between the transmitter, receiver, or surrounding scatterers.

$$T_c = \frac{1}{f_d} \quad (2.5)$$

Doppler spread broadens the received signal bandwidth due to relative motion, causes faster channel variations, and shorter coherence time. Rapid fluctuations produce fast fading, while slower changes from path loss and shadowing result in slow fading. Small-scale fading is often modeled statistically, with Rayleigh fading commonly used for environments without a dominant line-of-sight path

#### 2.4.1 Rayleigh Channel Fading

In a Rayleigh fading channel, there is no line-of-sight path, and the received signal consists of many reflected paths. by Central Limit Theorem, the sum of these independent components follows a complex Gaussian distribution with a zero mean, which models Rayleigh fading.

We can denote this as  $X \sim \text{CN}(0, \sigma^2)$ ,  $\sigma^2$  is the variance with channel envelope  $y = |x|$  and PDF expressed as

$$(f_{Y(y)}) = \frac{y}{\alpha^2} e^{-\left(\frac{y^2}{2\alpha^2}\right)} \quad (2.6)$$

#### 2.4.2 Wireless Channel Model

Modeling real wireless channels is difficult due to their complexity and variability. Empirical models, based on measurements, approximate typical scenarios using a complex random variable capturing path loss, shadowing, and small-scale fading. Standard models like ITU and 3GPP Spatial Channel Models simulate signal propagation in urban and rural environments. Double-directional models consider angles of arrival and departure, generating multiple rays with random delays, powers, and phases. Their combination reproduces effects such as antenna correlation, fading, and Doppler shifts.

For example, the Urban Macro (UMa) model simulates non-line-of-sight propagation in grid-like city layouts with base stations above buildings and users at ground level.

## **2.5 Ultra-dense wireless communication**

Cell splitting and network densification have long been fundamental approaches to boost capacity and enhance user experience in mobile networks. Recently, Ultra-Dense Networks (UDNs) have emerged as a critical solution for 5G, aiming to meet the IMT-2020 requirement of extremely high capacity up to 10 Mbps/m<sup>2</sup>. Simply put, UDNs deploy many more base stations (or access points) than traditional networks, creating a much denser network. Definitions vary: some consider UDNs as networks where base station density matches or exceeds user density [10]. Others define them by very short inter-site distances of just a few meters [35], while some describe UDNs as networks where further densification yields diminishing capacity gains due to interference.

In ultra-dense networks (UDNs), interference behaves very differently than in traditional cellular networks. Instead of a few dominant interferers, there are often many strong, but roughly equal, sources of interference, creating highly volatile conditions [23]. In conventional, sparsely deployed networks, user density usually exceeds base station (BS) density, especially during peak hours. Under heavy traffic, all BSs are active, and universal frequency reuse has long been considered optimal for maximizing capacity [1].

However, as networks become ultra-dense, some BSs may have no users but remain active, leading to slower SE growth and even eventual declines, indicating that BS density must be carefully optimized. Early studies often assumed a fixed path loss exponent, which can obscure some UDN effects [27], but the key insight remains: interference must be managed differently in ultra-dense scenarios.

Traffic fluctuations further complicate UDN operation. Since network demand varies by time and location, switching off underutilized BSs, so-called “BS sleeping becomes crucial for improving energy efficiency (EE) and reducing interference. In sparse networks with BS sleeping, spectral efficiency is proportional to BS density [10]. In contrast, in ultra-dense networks where BS density exceeds user density, SE increases only logarithmically with further densification. [28]

Effectively using the massive radio resources in UDNs is a challenging task. Poor resource allocation can worsen interference, create unbalanced loads, and increase power consumption. Moreover, in UDNs, local decisions have global consequences due to tight coupling between cells; radio resource management must consider the network as a whole rather than isolated areas [29] Providing wired

Providing backhaul to every BS in a UDN is often impractical; wireless self-backhauling consumes extra resources, adds interference, and increases latency. 5G maximizes energy efficiency by optimizing BS density, transmit power, antennas per BS, users per cell, and pilot reuse. Small cells improve EE but saturate at high density. The highest EE is achieved by combining UDNs with massive MIMO, where multiple antennas reduce interference, and serving many users lowers energy per user. [30].

**2.6 Multi-user MIMO**

Early cellular systems separated users by time, frequency, or code, assigning spectrum portions to limit interference. With the introduction of multi-antenna base stations, a new dimension of space became available. This allows the BS to distinguish signals to and from each user based on their spatial location, a concept known as Multi-User MIMO (MU-MIMO). By exploiting the spatial dimension, each user can access the entire spectrum, improving throughput without requiring additional spectral resources[18]. MU-MIMO requires multiple antennas at the BS, with spatial degrees of freedom limited by their number. The BS uses transmit beamforming, applying precoding weights to focus signals toward intended users and reduce interference while multi-antenna receivers can similarly enhance desired signals via receive beamforming. In a system with M BS antennas serving  $K \leq M$  single-antenna users, spatial multiplexing allows independent SISO-like streams per user, potentially increasing spectral efficiency linearly with K. Gains depend on the number of antennas and channel estimation accuracy.

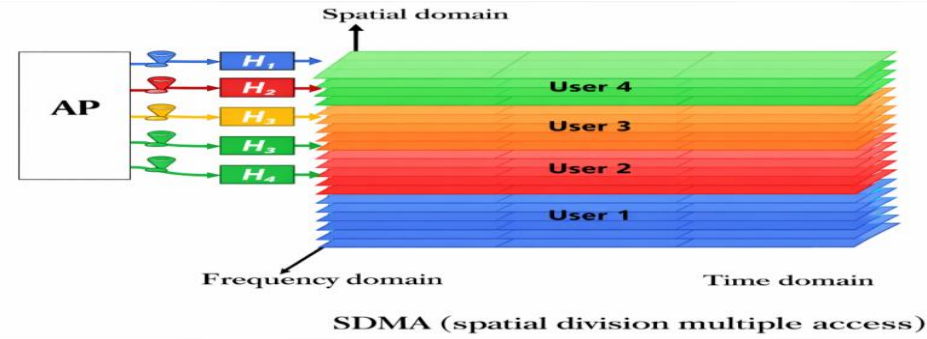


figure 2.21 MU-MIMO

## 2.7 Spatial multiplexing

Spatial multiplexing is a method that has been introduced to increase the data rate of a communication system. Rather than transmitting a single data stream, the data stream is broken into independent parallel data streams and sent concurrently over multiple spatial channels. Specialized processing techniques are employed at the receiver to recover these data sub-streams. Mathematically given by

$$d_{mul} = \lim_{y \rightarrow \infty} \left( \frac{R}{\log y} \right) \quad (2.7)$$

(bits/s/Hz) depends on SNR, and  $y$  is a function of SNR. The maximum spatial multiplexing gain of the MIMO channel ( $H$ ) is:

$$(d_{Mul})_{max} = \min((N_T, N_R)) \quad (2.8)$$

The MIMO channel's maximum spatial multiplexing gain,  $d_{mu}$  equals  $\min(N_T, N_R)$ , reflecting available degrees of freedom. Using multiple antennas at both ends increases throughput.

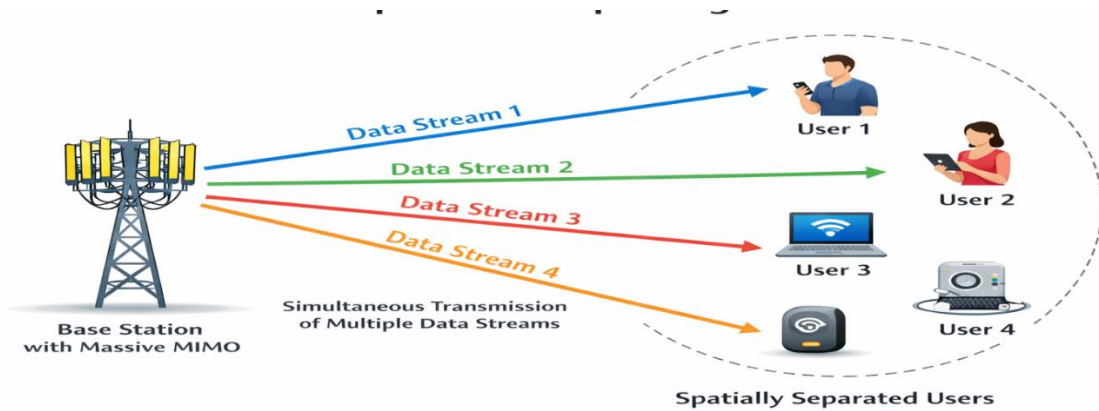


Figure 2.2 spatial multiplexing

## 2.8 Massive Multiple Input Multiple Output System (Massive MIMO)

One main goal of 5G is achieving 1000 times higher capacity per unit area than 4G., while keeping costs and energy consumption similar to today's cellular systems [31]. Increasing capacity requires more spectrum, denser base station deployment, and higher spectral efficiency. Massive MIMO

addresses the last factor by equipping each BS with many antennas (100+), enabling simultaneous communication with multiple users on the same resources. Using multipath propagation, it focuses energy on desired users while reducing interference, a technique known as beamforming. Massive MIMO is closely linked with 5G due to its significant performance gains. Massive MIMO utilizes the abundant spatial DoF provided by its antenna array. These DoFs allow the BS to spatially multiplex multiple users over the same frequency resources, effectively creating multiple independent channels. Focus transmitted energy toward intended receivers and reduce interference within and between cells.

Beamforming directs signals from multiple antennas with proper phase adjustments to coherently combine at the receiver. In this thesis, we define beam forming as applying the same phase shift across the entire system bandwidth. Pre-coding applies phase shifts across the bandwidth, with beamforming as a special case. Coherent processing across antennas lets downlink pre-coding focus signals on intended users and uplink combining separate signals from multiple users. Increasing the number of antennas allows for finer spatial focusing, which improves performance. [32].

Practical Massive MIMO usually uses TDD mode, where uplink and downlink share the same frequency at different times. Due to channel reciprocity, the base station can estimate the channel from the uplink and apply this information for downlink precoding.

Hardware is imperfectly reciprocal, but slow variations can be corrected through simple relative calibration using antenna coupling, often without extra equipment[31].

Advantages of operating in Time Duplex Division Mode:

- Only the BS needs accurate channel knowledge to process signals coherently.
- The overhead for channel estimation depends on the number of users, not the number of antennas, making the system scalable as more antennas are added.
- The quality of estimation improves as the number of antennas grows, given a known array correlation. Since wireless channels vary with time and frequency due to fading, channel estimation and data transmission are done within blocks where the channel is roughly constant. This ensures that the BS can accurately focus energy on the intended users and maintain high spectral efficiency. The coherence block is given by

$$\tau_c = B_c T_c \quad (2.9)$$

Transmission symbols set block size; Massive MIMO supports single- or multi-carrier modulation, with channel coherence affected by environment, mobility, and carrier frequency.

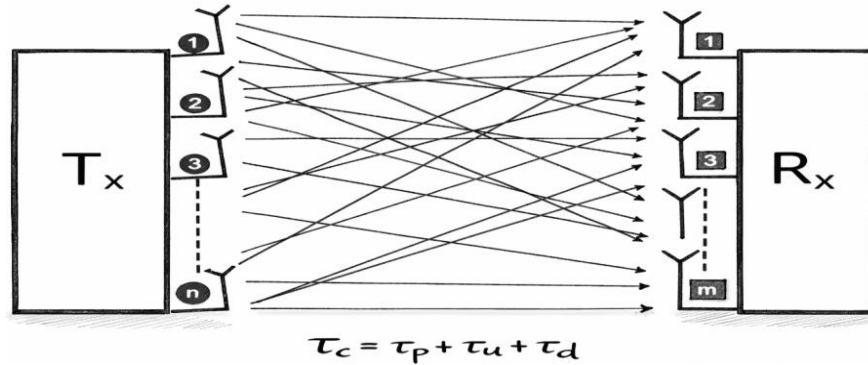


Figure 2.3 Concepts of massive MIMO technology

### 2.8.1 Features of Massive MIMO

The evolution of wireless communication is often described in terms of generations, each marking a major leap in capability. From the voice-focused 1G to the broadband multimedia 4G, each generation has been driven by the ever-growing demand for data and the increasing number of connected devices. 5G fundamentally redesigns wireless networks to support eMBB, mMTC, and URLLC for high-speed data, massive IoT, and ultra-reliable low-latency applications.

Massive MIMO, a key 5G technology, equips BSs with tens to hundreds of antennas to serve many users simultaneously via spatial multiplexing, greatly increasing network capacity. Inter-user interference is managed at the physical layer using precoding techniques like Zero-Forcing, based on accurate channel estimates from reference signals (CSI-RS, DM-RS) and algorithms such as MMSE. This enhances spectral efficiency by creating parallel spatial channels and improves energy efficiency by directing power toward intended users, reducing energy per bit. The key benefits of Massive MIMO over traditional MIMO include[19] Massive MIMO offers significant spectral and energy efficiency gains, abundant spatial degrees of freedom, strong performance with simple linear precoding (ZF, MRT, MMSE), and greater flexibility for efficiently serving many users.

### **2.8.2 Energy efficiency of Massive MIMO**

Energy efficiency is increasingly important in wireless communication, as improving spectral efficiency often raises energy consumption, increasing costs and CO<sub>2</sub> emissions. The radio access network consumes nearly 70% of mobile network power, making energy savings critical for both operators and uplink device battery life. Research focuses on energy-efficient techniques, but a trade-off exists: reducing energy may lower spectral efficiency, while maximizing throughput increases power use. Understanding this trade-off helps determine the energy needed for a target data rate or the achievable rate for a given energy budget.

In the literature, energy efficiency is the transmission bit rate per unit of transmit power (bits/Joule). The second definition considers the ratio of used power to the transmitted bit rate, expressed in Joules per bit [9][33]. In this thesis, the first definition is adopted, as it directly reflects energy consumption relative to the achieved data rate.

### **2.8.3 Massive MIMO Channel Estimation**

MU-MIMO can greatly improve spectral efficiency, but requires accurate, instantaneous CSI. While theoretical models assume perfect CSI at the BS and UEs, in practice, it must be estimated, with performance affected by the duplexing mode. In TDD systems, uplink and downlink use the same frequency at different times. Users send pilot signals, and the BS uses channel reciprocity to derive downlink CSI from uplink measurements. For this approach to work effectively, the wireless channel must remain stable for a sufficiently long period to cover both the uplink training phase and the subsequent downlink transmission. This means that the system depends on a sufficiently long coherence time [12].

In FDD systems, uplink and downlink use different frequencies, so channel reciprocity cannot be used. UEs must estimate the downlink channel and send it to the BS via feedback[22]. This feedback process can become a major bottleneck, especially in systems with large antenna arrays, because the amount of CSI that needs to be fed back grows rapidly. Accurate CSI is vital: the BS uses it to detect uplink signals and design downlink precoding. Uplink training assigns orthogonal pilots for BS channel estimation. Users only need their effective channel gain, not the full matrix, which can be obtained via a few beam-formed pilot symbols, reducing overhead.

#### 2.8.4 Massive MIMO Channel Model

Modeling of massive MIMO channel, three major classes of stochastic models are commonly used to evaluate system performance: Correlation-Based (CBSM), Parametric (PSM), and Geometry-Based (GBSM) stochastic models[22]. Each of these models captures different aspects of the radio propagation environment, and each comes with its own balance of accuracy, complexity, and practicality.

CBSMs are simple and computationally light, but ignore realistic propagation like spherical wavefronts. GBSMs model geometry and multipath more accurately but are costly. PSMs balance complexity and realism but are less used in Massive MIMO. CBSM variants include i.i.d. Rayleigh, correlated Rayleigh, and dispersive multipath, useful for analytical studies. While still simplified, this model allows researchers to examine the impact of spatial correlation and Doppler effects, making it particularly relevant for evaluating large-scale MIMO (LS-MIMO) deployments [12].

The dispersive multipath model adds realism by modeling multiple paths with different AoAs per user. Each path has a steering vector and attenuation, naturally separating users' signals, making it useful for studying inter-user and inter-cell interference in Massive MIMO [18].

Overall, CBSMs remain the most commonly used tools largely because of their analytical simplicity. They do not fully capture the spatial richness of Massive MIMO propagation environments. Consequently, accurately modeling Massive MIMO channels continues to be an open and active research challenge, especially as systems evolve toward larger antenna arrays, higher frequencies, and more dynamic environments.

### 2.8.5 Massive MIMO Data Transmission Protocol

Massive MIMO typically operates in TDD mode. Within each coherence interval, channel estimation (via uplink and downlink training), uplink data transmission, and downlink data transmission are performed.

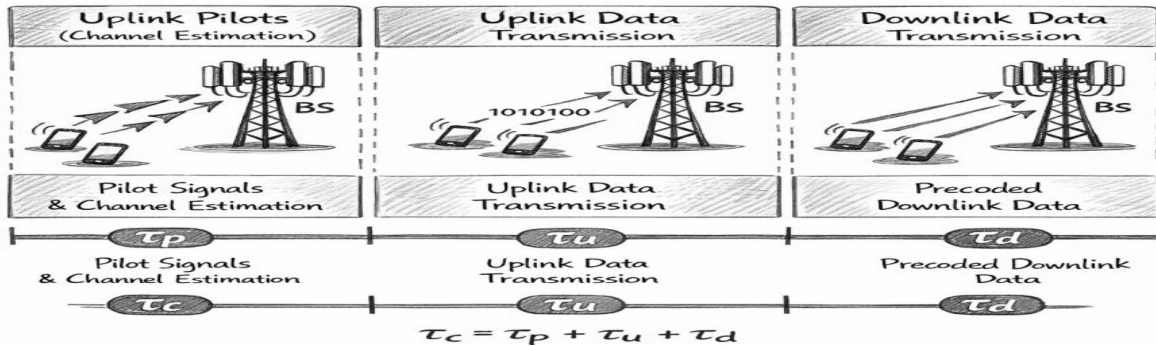


Figure 2.4 TDD with coherence interval

### 2.8.6 Massive MIMO Uplink Data Transmission

In the uplink phase, users transmit simultaneously over shared resources, and the BS applies channel estimates with linear combining for detection.

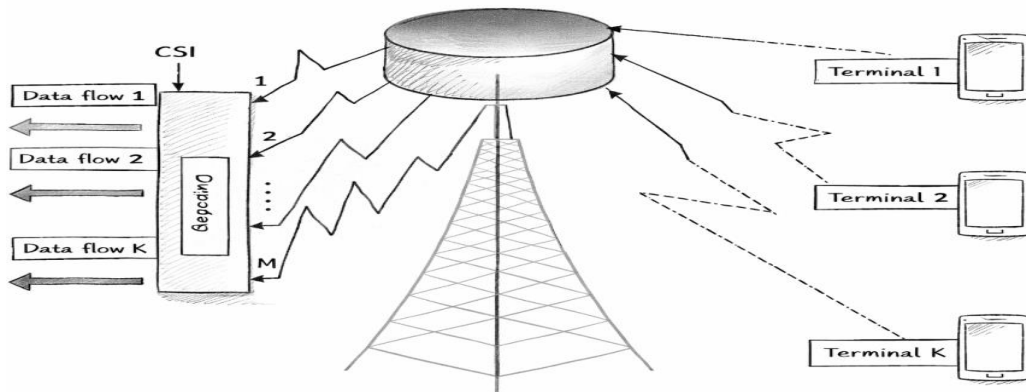


Figure 2.5 massive mimo uplink

### 2.8.7 Massive MIMO Downlink Data Transmission

For the downlink, the BS transmits to all  $K$  users simultaneously using the same time-frequency resources. It applies channel estimates to precode the user symbols into  $M$  signals, which are sent through the  $M$  antennas.

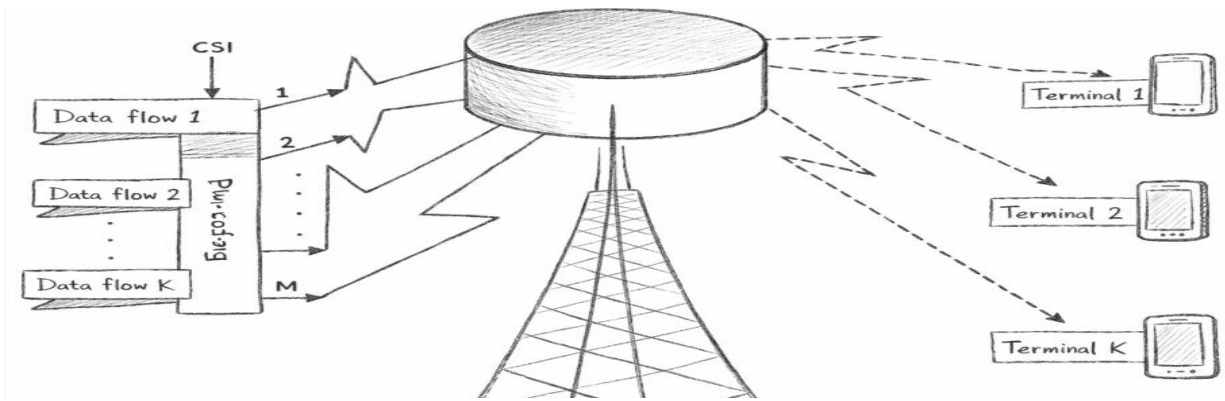


Figure 2.6 massive mimo down link

### 2.8.8 Pre-coding techniques in massive MIMO

Linear processing at the base station (BS) plays a central role in enabling reliable payload transmission in Massive MIMO systems. Pre-coding, in particular, provides two essential benefits: it mitigates inter-user interference and it shapes the transmitted signal through beam-forming so that energy is directed toward the intended users. Broadly, pre-coding techniques fall into two categories: nonlinear and linear schemes. While nonlinear pre-coding is capable of fully eliminating both interference and shaping beams with high precision, linear pre-coding primarily focuses on reducing inter-user interference [14].

In practical wireless communication environments, the geographic distribution of users means that their transmitted signals seldom arrive simultaneously at the BS[22]. This misalignment makes it difficult to cancel inter-user interference solely through multi-user detection. As a result, pre-coding becomes indispensable for maintaining system performance, especially in multi-user scenarios where interference can significantly degrade throughput.

Nonlinear precoding can be optimal, but is too complex for large systems. Linear precoding offers low complexity and strong performance, making it practical and effective for Massive MIMO with many antennas [13][29].

### **2.8.9 Linear pre-coding schemes in MIMO**

Linear processing at the BS separates overlapping uplink signals from  $K$  users over  $M$  antennas. MR maximizes gain, ZF cancels interference, and MMSE balances both. This creates cleaner channels and, as  $M$  grows, leads to channel hardening. Uplink combining and downlink precoding are linked via uplink–downlink duality[22]. In TDD systems, where the same frequency band is used for both directions, the uplink and downlink channels are reciprocal. This allows the BS to apply the same principles of MR, ZF, or MMSE to focus downlink signals on their intended users while reducing interference.

In classical multi-user MIMO theory, the best-performing uplink detection method is Successive Interference Cancellation (SIC), which can theoretically achieve the maximum rate [24]. However, SIC is far too computationally demanding for practical, large-scale systems. This limitation has driven the adoption of simpler, but still powerful, linear detection techniques such as MR/MRC, ZF, and MMSE [34][24][35]. For example, [29] provides asymptotic SINR results for MRC (uplink) and MRT (downlink), while [24] offers exact uplink performance analysis for systems with arbitrarily many antennas. These studies consistently show that linear receivers can fully capitalize on the large antenna arrays of Massive MIMO while keeping implementation complexity manageable.

Among these linear methods, ZF receivers are often preferred because they completely remove intra-cell interference, allowing the system to perform well without requiring an excessively large number of antennas. Although the MMSE receiver generally provides the strongest performance, the advantage over ZF becomes negligible at high SINR values [3]. MMSE also requires more detailed statistical knowledge and introduces a higher computational load, which is not always desirable for large-scale deployments. Because of its strong performance complexity balance, ZF emerges as an especially appealing choice for Massive MIMO systems, and therefore, it is adopted in this thesis [9].

Some earlier analyses, such as [26]. With perfect CSI at both transmitter and receiver, exact performance can be determined. In practice, CSI is imperfect and estimated at the BS using uplink pilot signals from the users [36]. The Least Squares (LS) estimator is simple but performs poorly

under strong inter-cell interference. The MMSE estimator offers much better accuracy and is widely used in modern Massive MIMO systems [37].

Once the BS has obtained its channel estimates, it applies a linear detection technique such as the ZF method used in this thesis to recover the users' data during the uplink transmission phase.

## 2.9 Limitations of Massive MIMO

Despite its significant advantages, Massive MIMO faces several challenges that must be addressed. The main issues are outlined below;

### 2.9.1 Pilot Contamination

Up to this point, the discussion has focused on single-cell systems with perfect CSI. Real cellular networks, however, consist of many interacting cells that must share limited time-frequency resources. As a result, both single-cell systems with imperfect CSI and multi-cell environments must be examined. In multi-cell networks, the channel coherence interval is too short to assign fully orthogonal pilot sequences to every user in every cell[38] . Consequently, pilots must be reused across cells, causing the channel estimates in one cell to be corrupted by pilot signals transmitted in neighboring cells. This phenomenon, known as pilot contamination, degrades system performance and represents one of the most fundamental limitations of large-scale MIMO systems. Importantly, pilot contamination persists even as the number of BS antennas grows without bound.

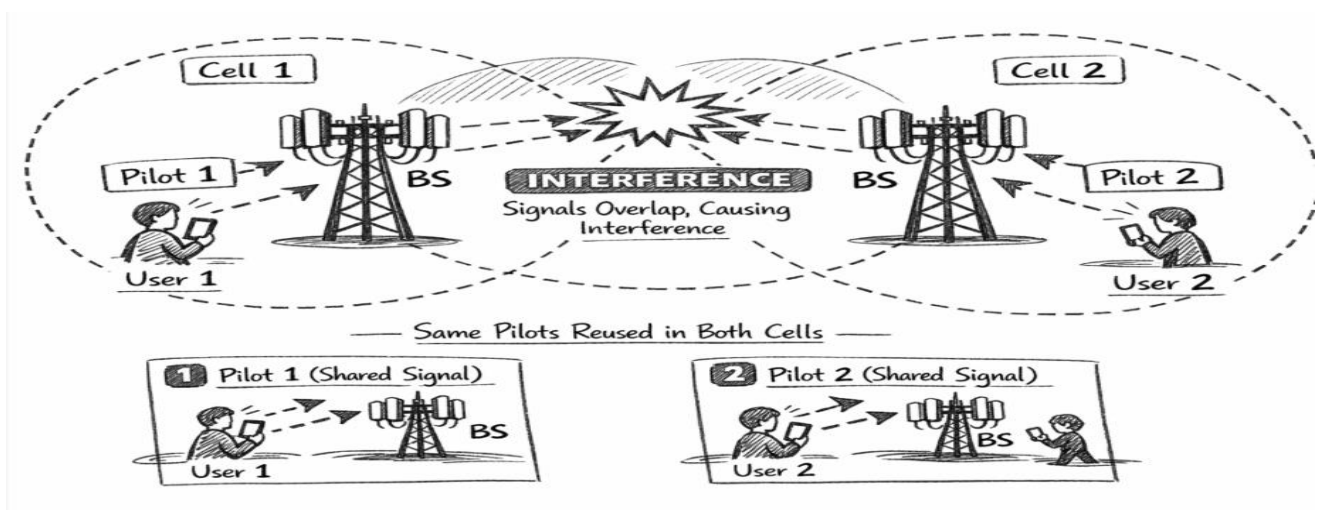


Figure 2.7 Pilot contamination in massive mimo

Because of its impact, extensive research has focused on mitigating pilot contamination. Notable approaches include eigenvalue-based channel estimation, pilot decontamination techniques, and pre-coding strategies specifically designed to suppress contamination effects, as discussed in [24].

### 2.9.2 Unfavorable Propagation

Massive MIMO achieves its best performance under favorable propagation, where user signals arrive at the base station in distinct spatial directions. In practice, limited scattering or shared scatterers can cause channel overlap, reducing user separability. Distributing base-station antennas over a wider area helps increase spatial diversity and mitigate this issue.

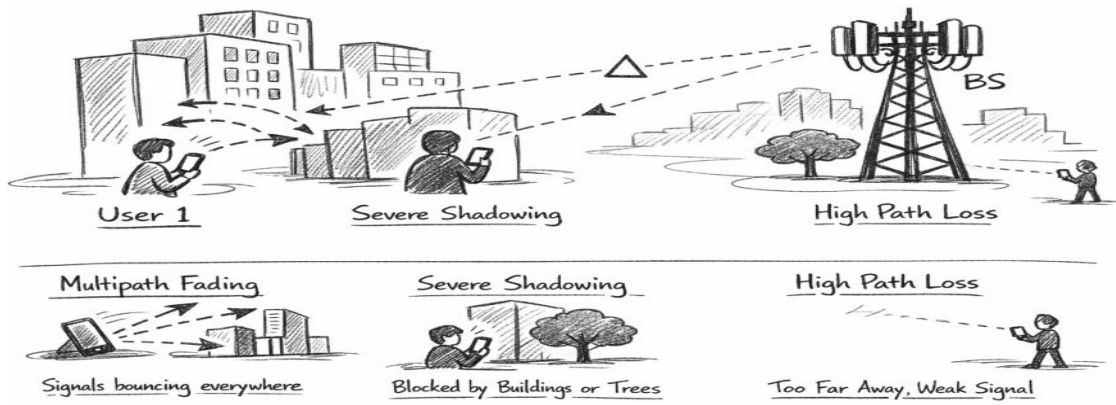


Figure 2.8 Unfavorable propagation in massive MIMO

A key limitation of earlier Massive MIMO studies is the simplified treatment of power consumption, often neglecting circuit power or modeling it as a constant. In practice, total power consumption scales with system parameters such as the number of antennas, number of users, and signal processing complexity. Therefore, analyzing the tradeoff between energy efficiency and spectral efficiency requires a scalable and realistic power model. Recent research addresses this by incorporating system-dependent power consumption, enabling a more accurate assessment of how design parameters influence overall energy efficiency.

### 2.9.3 Energy efficiency techniques in 5G wireless communications

Modern wireless networks consume substantial power, and this demand will increase with the expansion of connected devices and IoT. Energy efficiency improvements focus on three main aspects: energy-efficient architectures (e.g., heterogeneous networks with macro/small cells and

relays), intelligent resource management (optimized power and spectrum allocation), and low-power radio technologies, including multi-RAT selection.

Massive MIMO and network densification are key enablers of green communications. Massive MIMO employs large antenna arrays to spatially focus energy, reduce radiated power, and support many users simultaneously with high energy efficiency, even under imperfect CSI or hardware impairments.

As 5G targets traffic levels up to 1000× higher than 4G and increasingly integrates renewable energy sources with limited real-time availability, energy efficiency becomes fundamental.

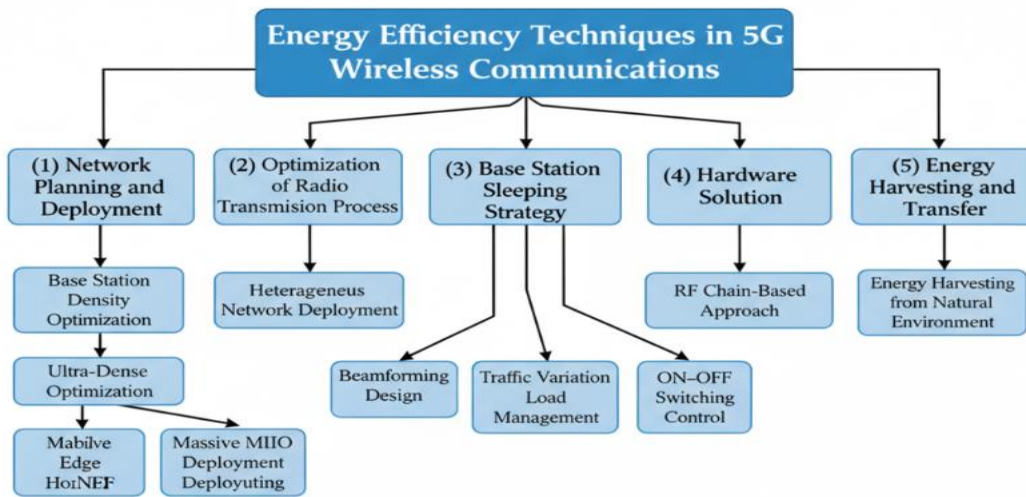


Figure 2.9: Overview of Energy Efficiency Techniques in Wireless Communications

### 2.9.4 Massive MIMO Power Consumption

The energy usage of a base station in the ICT sector industry increasingly deploys Massive MIMO in single- and multi-cell networks, as large antenna arrays improve uplink and downlink power efficiency. With hundreds of antennas, base stations can serve many users simultaneously using spatial degrees of freedom. As antennas increase, user channels become nearly orthogonal, reducing interference and enabling spatial multiplexing, which boosts throughput and link reliability. Uplink transmit power can be lowered, benefiting battery-limited devices, but base station power consumption rises due to RF chains, signal processing, cooling, and amplifiers. Simplified models treating total power as transmit plus fixed circuit power are inaccurate for large arrays; in reality, circuit and processing power scale with both antennas ( $M$ ) and users ( $K$ ), and must be carefully

modeled for energy-efficient design. In a true Massive MIMO environment where both  $M$  and  $K$  are large and all antenna elements are jointly processed, this scaling cannot be ignored. A realistic, scalable power consumption model is therefore essential to provide meaningful design guidelines for maximizing energy efficiency in next-generation wireless networks.

### **2.9.5 System Parameters in Massive MIMO**

Studies have explored how the number of base station (BS) antennas,  $M$ , affects energy efficiency (EE) in Massive MIMO systems [3]. In particular, research on multi-user MIMO uplink systems has shown that carefully managing power allocation can significantly boost EE, sometimes even by selectively switching off certain user equipment (UEs) [39][29][3]. Similarly, other studies have found that EE behaves as a concave function of both the number of BS antennas and the user rates in the uplink [15], while in the downlink, EE also follows a concave relationship with  $M$  [24]. A comparable result holds for the number of active users,  $K$ , in [40].

However, most of these results come from simulations, which offer useful insights but do not provide a complete picture of how EE truly responds to all system parameters under realistic conditions. For example, while some works suggest letting  $K$  grow very large or even approach infinity, which yields higher EE, they often ignore the overhead signaling required for channel estimation, making such conclusions unrealistic [41].

Another critical factor in the power utilized by a base station is the power amplifier (PA). A BS's power consumption can be broadly divided into three parts: the pre-transceiver block, the transceiver block, and the PA itself [40]. Among these, the PA often dominates because its consumption scales with the transmit power. One of the main sources of power loss in the PA is due to linearity requirements. The performance and efficiency of a PA are highly dependent on processing signals characterized by high peak-to-average power ratios (PAPR), which are common in modern modulation schemes like OFDM.

To mitigate these losses, advanced PA designs such as the Doherty Power Amplifier (DPA) are often used. The DPA combines a carrier amplifier and a peak amplifier: the peak amplifier only activates when the carrier amplifier reaches saturation, ensuring more efficiency even at large back-off points (BOPs) [29]. A conventional two-stage DPA can achieve peak efficiency at around 6 dB of BOP, and efficiency can be further improved by adding more peak amplifiers. Proper management of PAPR

and PA efficiency is therefore crucial for reducing BS power consumption while maintaining system performance.

In a practical MIMO system, the uplink and downlink share bandwidth  $B$ , where a base station with  $M$  antennas serves  $K$  single-antenna users sequentially. The channel exhibits flat fading and remains constant within each coherence block defined by coherence bandwidth  $B_C$  and time  $T_C$ . The system uses TDD with perfect BS–UE synchronization, and the coherence block is divided between uplink and downlink such that  $ul+dl=1$ . [24], [40]. Uplink transmission occurs first and consists of  $ul$  symbols, followed by  $dl$  symbols for downlink. Pilot signals are sent in both directions.

In TDD, uplink pilots provide channel estimates for the BS, which are reused for downlink precoding due to channel reciprocity, ensuring consistent handling of  $M$  antennas and  $k$  users..

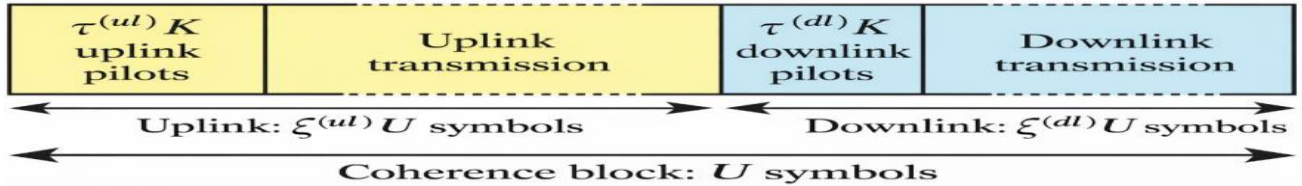


Figure 3: TDD protocol

Since users are scheduled in a round-robin manner, their locations are treated as random variables drawn from a spatial distribution  $f(x)$ , which defines the coverage area characteristics. The large-scale fading is assumed identical across all BS antennas, as the UE–BS distance is much larger than the inter-antenna spacing. The analysis remains general with respect to user distribution, while a symmetric scenario is adopted for simulations.

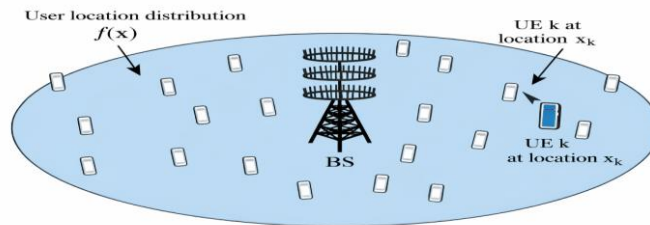


Figure 3.1 generic multiuser MIMO

User equipment (UEs) is uniformly distributed in a circular cell with radius  $d_{\max}$  maintaining a minimum distance  $d_{\min}$  and their spatial distribution is characterized by a density function.

$$f_x = \begin{cases} \frac{1}{\pi(d_{\max}^2 - d_{\min}^2)} & d_{\min} \leq \|x\| \leq d_{\max} \\ 0 & \text{otherwise} \end{cases} \quad (2.10)$$

For over large-scale fading pathloss considered

$$l_x = \frac{d}{\|x\|^\kappa} \quad \text{for all } \|x\| \geq d_{\min} \quad (2.11)$$

$\kappa \geq 2$  denotes the path-loss exponent, and  $\bar{d} > 0$  sets attenuation at  $d_{\min}$  [42].

Recent works study EE in Massive MIMO and SCNs, showing SCN EE rises with BS density only below a circuit power threshold, and EE–SE trade-offs for Massive MIMO have been analyzed [24], [40] Circuit power effects on EE–SE were given in derived in closed form, applicable only when ICI is absent in a single cell

### 2.9.6 Massive MIMO Channel Model and Linear Processing

Massive MIMO achieves its goal when all  $M$  antennas located at the base station maintain enough distance to create uncorrelated propagation components linking base station antennas between base station antennas and single antenna user equipment.

The Massive MIMO channel vector is expressed by

$$h_k = [h_{k,1}, h_{k,2}, \dots, h_{k,m}]^T \in \mathbb{C}^{M \times 1} \quad (2.12)$$

The channel vector  $h_k$  represents the instantaneous link between the  $n$ -th BS antenna and the  $k$ -th UE. Under Rayleigh fading, it follows a zero-mean complex Gaussian distribution with covariance  $\beta_{(xk)} \mathbf{I}_M$ , capturing both small- and large-scale fading. Linear processing is used for uplink detection and downlink precoding, assuming perfect CSI at the base station. The uplink linear receive combining matrix is denoted by

$$G = [g_1, g_2, \dots, g_k] \in M \times K \quad (2.13)$$

With the column being assigned to the  $k^{\text{th}}$  UE. The MRC, ZF, and MMSE processing are considered for uplink detection, which gives

$$G = \begin{cases} H & \text{for MRC,} \\ H(H^H H)^{-1} & \text{for ZF,} \\ (HP^{ul} H^H \alpha^2 I_m)^{-1} H & \text{for MMSE,} \end{cases} \quad (2.14)$$

Here,

$$H = [H_1, H_2, \dots, H_K] \quad (2.15)$$

It includes all user channel vectors, while  $\sigma^2$  represents the noise variance measured in Joules per symbol.

$$p^{(ul)} = \text{diag}(p_1^{(ul)}, p_2^{(ul)}, \dots, p_k^{(ul)}) \quad (2.16)$$

The parameter  $p_i^{(ul)} \geq 0$  represents the uplink transmit power allocated to user  $i$  (in Joule/symbol), for  $i=1, 2, \dots, K$ . In the downlink phase, linear precoding techniques such as MRT, ZF, and MMSE are employed [10]. The pre-coding is given by matrix.

$$V = [V_1, V_2, \dots, V_K] \in \mathbb{C}^{M \times K} \quad (2.17)$$

$$V = \begin{cases} H & \text{for MRC,} \\ H(H^H H)^{-1} & \text{for ZF,} \\ (HP^{ul} H^H \alpha^2 I_m)^{-1} H & \text{for MMSE,} \end{cases} \quad (2.18)$$

Setting  $V=G$  simplifies computation but is optional. The system aims to provide a uniform gross rate  $R^-$  for all active UEs, with  $\zeta_{ul} R$  and  $\zeta_{dl}$  as the uplink and downlink rates.

### 2.9.7 Uplink in Massive MIMO System

The signal received by the base station is expressed as

$$y_{jk} = \sum_{l=1}^L \sum_{k=1}^K \sqrt{p_{li}} h^H x_k v_{li} s_{li} + n_{jk} \quad (2.19)$$

Where:  $\mathbf{h}_k \in \mathbb{C}^{M \times 1}$  is the channel vector of user  $k$ .  $x_k$  is uplink symbol of user  $k$ ,  $E[|x_k|^2] = p_k$  and  $n \sim \text{CN}(0, \sigma^2 \mathbf{I})$

Base station applies combiner

$$\mathbf{v}_k^H \hat{x}_k = \mathbf{v}_k^H \mathbf{y} \quad (2.20)$$

With Gaussian codebooks, linear processing, and perfect CSI [42]. The achievable uplink rate in (bit/second) of the  $k$ th UE is

$\zeta^{(ul)}$  is the fraction of uplink transmission. Likewise,

$$R_k^{ul} = \zeta^{(ul)} \left( \mathbf{1} - \frac{\tau^{ul} k}{U \zeta^{(ul)}} \right) R_k^{UL} \quad (2.21)$$

$$R_k^{ul, per} = B \log_2(\mathbf{1} + SINR_k^{UL}) \text{ [bits/s]} \quad (2.22)$$

$$SE_K^{UL} = \left( \mathbf{1} - \frac{\tau_p}{\tau_c} \right) \log_2(\mathbf{1} + SINR_K^{UL}) \text{ [bits/s/Hz]} \quad (2.23)$$

$$SINR_k^{ZF, imp} = \frac{(m-k) p_k \gamma_k}{\sum_{i \in p_k/k} (M-K) p_i \gamma_i + \delta^2} \quad (2.24)$$

$$\gamma_k = \frac{\tau_p p_k \beta_k^2}{\tau_p \sum_{i \in p_k} p_i \beta_i + \delta^2} \quad (2.25)$$

$$SINR_k^{mrc, imp} = \frac{M p_k \gamma_k}{\sum_{i=1}^K p_i \beta_i + \sum_{i \in p_k/k} p_i \gamma_i + \delta^2} \quad (2.26)$$

$$SINR_k^{ZF, per} = \frac{p_k (m-k) \beta_k}{\delta^2} \quad (2.27)$$

$$R^{(-ul)} = B \log_2 \left( \mathbf{1} + \frac{p_k^{ul} |gk^H h_k|^2}{\sum_{l=k \neq k} p_{ul} |gk^H h_l|^2 + \sigma^2 \|gk\|^2} \right) \quad (2.28)$$

The uplink gross rate of the  $k$ th UE is the transmission rate (in bits/s) excluding overhead, aiming to maintain the same gross rate.

$$R_k^{(-ul)} = R^- \quad \text{for } k = 1, 2, \dots, K \quad (2.29)$$

Mechanism from [42]. This equal-rate condition holds only when the uplink power allocation vector satisfies it.

$$p^{(ul)} = [p_1^{(ul)}, p_2^{(ul)}, \dots, p_K^{(ul)}]^T \quad (2.30)$$

$$p^{(ul)} = \sigma^2 (D^{ul})^{-1} \mathbf{1}_K \quad (2.31)$$

Where the  $(k, k)$ th element of  $D^{ul} \in \mathbb{C}^{K \times K}$  is given by

$$[D^{ul}]_{kl} = \begin{cases} \frac{|gk^h h_k|^2}{(2^{R/B} - 1) \|g_k\|^2} & \text{for } MRC \\ -\frac{|gk^h h_k|^2}{\|g_k\|^2} & \text{for } zf \end{cases} \quad (2.32)$$

Average uplink PA power includes transmitted power and PA dissipation.

$$P_{Tx}^{ul} = \frac{B \zeta^{(ul)}}{\eta^{(ul)}} E \{ \mathbf{1}_K^t p^{(ul)} \} = \partial^2 \frac{B \zeta^{(ul)}}{\eta^{(ul)}} E \{ \mathbf{1}_K^t D^{(ul)-1} \} \mathbf{1}_K \quad (2.33)$$

$\eta^{(ul)}$  (0–1) is the UE PA efficiency.

If  $R^-$  is unsupportable,  $P_{ul}$  may become negative, detectable via the spectral radius. This occurs only under interference, not with ZF and perfect CSI, where  $P_{Tx}^{(ul)}$  is computed in closed form.

$M \geq K + 1$ , zf is applied and the gross rate is given as

$$R^- = B \log(\rho(M - K)) \quad (2.34)$$

$\rho$ , proportional to SINR, determines the RF power ( $P_{ul-ZF}$ ) required per UE, considering user distribution and channel conditions.

$$P_{T_x}^{ul-ZF} = \frac{B\zeta^{(ul)}}{\eta^{(ul)}} \partial^2 \alpha S_X K \quad (2.35)$$

$$S_X = E_x \{(\mathbf{1}(x))^{-1}\} \quad (2.36)$$

### 2.9.8 Downlink in Massive MIMO System

The downlink transmit signal is given by

$$X_j = \sum_{K=1}^K \sqrt{P_{JK}} W_{JK} S_{JK} \quad (2.37)$$

Where:  $W_k \in \mathbb{C}^{M \times 1}$  is the precoding (beamforming) vector for user  $k$ ,  $S_k$  is the data symbol for user  $k$ , with  $E[|s_k|^2] = p_k$ , and  $x$  is the transmitted signal vector.

Signal received at user  $k$  is given by

$$y_k = h_k^H x + n_k = h_k^H \sum_{i=1}^k w_i s_i + n_k \quad (2.38)$$

$$y_k = h_k^H w_k s_k + \sum_{i \neq k} h_k^H w_i s_i + n_k \quad (2.39)$$

where  $h_k^H w_k s_k$  desired signal and  $h_k^H w_i s_i$  is inter- user interference

Achievable Downlink Rate (General Form) is given by

$$R_K^{dl} = \left(1 - \frac{\tau_\rho}{\tau_c}\right) B \log_2(1 + SINR_K^{dl}) \quad (2.40)$$

ZF with perfect CSI,

$$W = H(H^H H)^{-1} \quad (2.41)$$

Asymptotically:

$$SINR_k^{ZF,perf} \approx \frac{p_k(M-K)\beta_k}{\delta^2} R_k^{dl} = (1 - \frac{\tau_p}{\tau_c}) B \log_2(1 + SINR_k^{DL}) \quad (2.42)$$

ZF with imperfect CSI

$$,W = H(H^H H)^{-1} \quad (2.43)$$

$$SINR_k^{ZF,IMP} = \frac{p_k(M-K)p_k\gamma_k}{\sum_{i \in p_k/k} (M-K)p_i\gamma_i + \delta^2} \quad (2.44)$$

A normalized pre-coding vector  $v_k/\|v_k\|$  and  $R_k^{-(dl)}$  The downlink signal to the  $k^{\text{th}}$  is assigned a transmit power of  $\zeta^{(dl)}$  (in Joule/symbol). In [10], assuming Gaussian codebooks and perfect CSI, the achievable downlink rate (in bits/second) of the  $k^{\text{th}}$  UE with linear processing

$$R_k^{(dl)} = \zeta^{(dl)} \left( \mathbf{1} - \frac{\tau^{(dl)}k}{u\zeta^{(dl)}} \right) R_k^{-(dl)} \quad (2.45)$$

Where the  $\left( \mathbf{1} - \frac{\tau^{(dl)}k}{u\zeta^{(dl)}} \right)$  It includes downlink pilot overhead and represents the gross data rate (in bit/s) given by[43].

$$R_k^{-(dl)} = B \log \left( \mathbf{1} + \frac{p_k^{dl} \frac{|h_K^H v^k|^2}{|v^k|^2}}{\sum_{l=1, l \neq k}^k p_l^{dl} \frac{|g_K^H h_l|^2}{\|v_l\|^2 + \delta^2}} \right) \quad (2.46)$$

The average PA power is defined as

$$p_{Tx}^{dl} = \frac{B\zeta^{(dl)}}{\eta^{(dl)}} \sum_{k=1}^k E\{p_t^{(dl)}\} \quad (2.47)$$

Here,  $0 < \eta^{(dl)} \leq 1$  denotes the base station PA efficiency. Under the equal-rate condition  $R_k^{(dl)} = R^*$  for all  $k$ , the power allocation vector follows.

$$\mathbf{p}^{(dl)} = \left[ p_1^{(dl)}, p_2^{(dl)}, \dots, p_k^{(dl)} \right]^T \quad (2.48)$$

must be computed as

$$\mathbf{p}^{(dl)} = \partial^2 \left( \mathbf{D}^{(dl)} \right)^{-1} \mathbf{1}_K \quad (2.49)$$

Where the (k)th element of  $\mathbf{D}^{(dl)} \in \mathbb{C}K \times K$  is given by

$$\left[ \mathbf{D}^{(dl)} \right]_{k_1} = \begin{cases} \frac{|\mathbf{h}_k^H \mathbf{v}^k|^2}{(2^{-R/B} - 1) \|\mathbf{V}_K\|^2} & \text{for } k=1 \\ \frac{|\mathbf{h}_k^H \mathbf{v}^k|^2}{\|\mathbf{V}_K\|^2} & \text{for } k \neq 1 \end{cases} \quad (2.50)$$

Putting

$$\mathbf{p}^{(dl)} = \partial^2 \left( \mathbf{D}^{(dl)} \right)^{-1} \mathbf{1}_K \quad (2.51)$$

$$p_{T_x}^{dl} = \partial^2 \frac{B \zeta^{(dl)}}{\eta^{(dl)}} \mathbb{E} \left\{ \mathbf{1}_k^T \mathbf{D}^{(dl)^{-1}} \mathbf{1}_k \right\} \quad (2.52)$$

If the same scheme is used for precoding and combining (G=), then dl =ul; user-specific powers differ, but total uplink and downlink PA powers remain equal (up to a factor).  $\frac{\zeta^{(ul)}}{\eta^{(ul)}}$  and  $\frac{\zeta^{(dl)}}{\eta^{(dl)}}$ . This is a consequence of the well-known uplink-downlink duality. Like the uplink, the following result can be proved for ZF in the downlink

If a ZF pre-coding is devised with  $M \geq K + 1$ , then the average downlink PA power

$$p_{T_x}^{dl-ZF} = \frac{B \zeta^{(dl)}}{\eta^{(dl)}} \partial^2 p S_x K \quad (2.53)$$

Where  $S_x$  is the  $p \eta = \left( \frac{\zeta^{(ul)}}{\eta^{(ul)}} + \frac{\zeta^{(dl)}}{\eta^{(dl)}} \right)^{-1}$

for both uplink and down link power is added up to

$$P_{TX}^{ZF} = p_{Tx}^{(ul-ZF)} + p_{Tx}^{(dl-ZF)} = \frac{B\sigma^2 p_{s_x} k}{\eta} \quad (2.54)$$

## 2.9 5 Massive MIMO Systems Existing Power Consumption Model

Energy efficiency (EE) is the ratio of total data rate (bits/s) to power consumption (W), indicating rate per unit energy (bits/J) [42][13][24]. The total energy efficiency in a multi-user system includes both uplink and downlink, considering circuit power ( $P_{CP}$ ) in addition to transmit power, and is expressed as follows

$$EE = \frac{\sum_{k=1}^K (E\{R_k^{(ul)}\} + E\{R_k^{(dl)}\})}{P_t^{(ul)} + P_t^{(dl)} + P_{cp}} \quad (2.55)$$

In most EE studies,  $P_{CP} = P_{FIX}$  represents fixed power for site cooling, control signaling, backhaul, and baseband processing[38]. Assuming fixed  $P_{CP}$  is inaccurate for optimizing M and K, as ZF rates grow logarithmically with M, falsely suggesting unbounded EE. Each antenna adds circuit power and processing complexity, so accurate  $P_{CP}$  modeling is crucial for energy-efficient system design.

Based on the circuit power consumption model, EE is defined as [42][34]

$$EE = \frac{\sum_{k=1}^K (E\{R_k^{(ul)}\} + E\{R_k^{(dl)}\})}{P_t^{(ul)} + P_t^{(dl)} + P_{cp(M,R,K)}} \quad (2.56)$$

The research uses this model to develop a proper model which transforms three key design elements into model M. The solution to the problem uses ZF precoding schemes Dinkel Bach fractional programming which the thesis presents.

# CHAPTER THREE

## ENERGY EFFICIENCY OPTIMIZATION FOR 5G ULTRA DENSE WIRELESS COMMUNICATION NETWORKS USING MASSIVE MIMO SYSTEMS

### 3.1 System model

This thesis studies energy efficiency optimization in ultra dense 5G wireless networks using Massive MIMO. It reviews prior work and considers a cellular system where each base station has  $M$  antennas serving  $K$  uniformly distributed users. Energy efficiency is defined as the ratio of average data rate to total power consumption, and system parameters are optimized to maximize it. In mathematics, it is defined as [42][13][24].

$$EE = \frac{\text{Throughput}}{\text{powerconsumption}} \left( \frac{\text{bits / cell}}{\text{w / cell}} \right)$$

$$EE = \frac{\sum_{k=1}^K \left( E\{R_k^{(ul)}\} + E\{R_k^{(dl)}\} \right)}{p_t^{(ul)} + p_t^{(dl)} + p_{cp(M,R,K)}} \quad (3.1)$$

This is measured in bits/joule. This work evaluates energy efficiency by computing system throughput to total power consumption, which includes both circuit and transmit power. The accuracy of power modeling determines energy efficiency optimization. The system design consists of three essential parameters, which define base station antennas ( $M$ ), active users ( $K$ ), and throughput ( $R$ ) requirements. We examine how energy efficiency changes with these factors while measuring circuit and total power during uplink and downlink activities. Data rates are computed using zero-forcing precoding, which assumes that users distribute uniformly throughout a circular cell while experiencing uncorrelated Rayleigh flat fading. The efficiency optimization uses standard settings in MATLAB simulations which implement the Dinkel Bach algorithm and analytical ZF processing for both perfect and imperfect CSI conditions in a single-cell scenario.

The complete workflow diagram is shown below.

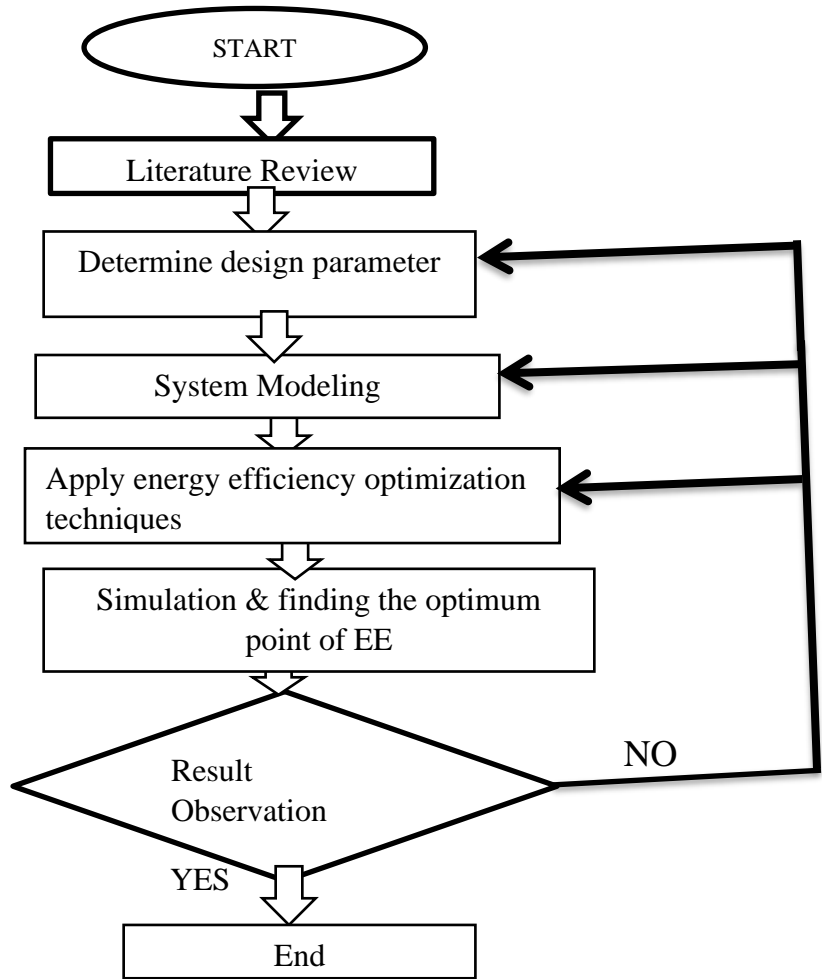


Figure 3.1: Overall work follow chart

Energy efficiency depends on both throughput and the usage of total power. According to the circuit power model, it can be improved by increasing throughput while reducing power, reducing both, or increasing both. In practice, systems often increase throughput along with power consumption, achieving higher overall energy efficiency.

The technology of Massive MIMO demonstrates the capability to increase throughput while delivering substantial energy savings. The complete power consumption of Massive MIMO networks must receive thorough examination starting from their fundamental circuit power consumption model because this aspect determines the total system energy efficiency.

### 3.2 Evaluation of Total Power Consumption in Massive MIMO Systems

The whole power consumption of the Base stations has fixed power consumption for operations and signaling, and variable power that rises with traffic. Fixed power leads to energy waste in low-traffic or rural areas, so accurate power modeling is needed for detailed system analysis. EE. Mathematically, the total power consumption,  $P_T$ , is equal to the sum of transmit power and circuit power, thereby creating the basis of the model detailed in Equation (3.1) to describe energy efficiency [44].

$$P_T = P_{TX} + P_{TC} \quad (3.2)$$

The transmit average power ( $P_{TX}$ ) and circuit power ( $P_{CP}$ ) together give total power consumption in watts. Adding antennas increases data rate, but also power use, with circuit power scaling with  $M$  and  $K$ . Total RF power ( $P_{TX}$ ) is defined in Equation (2.37), with  $\eta$  representing the averaged PA efficiency over uplink and downlink.

### 3.3 Massive MIMO Circuit-Level Power Consumption

The amount of energy that is consumed by separate analog components as well as digital signal processing, is usually called circuit power. Based on prior works of [42]. A new proposed circuit power consumption model for Massive MIMO systems is

$$P_C = P_{FIX} + P_{TC} + P_{CE} + P_{C/D} + P_{BH} + P_{LP} \quad (3.3)$$

The fixed power ( $P_{FIX}$ ) defines a fixed value that accounts for the total power needed to operate the site cooling systems and control signal processing, and the power consumption that does not depend on backhaul systems and baseband processors.  $P_{TC}$  denotes transceiver chain power,  $P_{CE}$  the channel estimation power per coherence block,  $P_{CD}$  the coding/decoding power,  $P_{BH}$  the load-dependent backhaul power, and  $P_{LP}$  the BS linear processing power.

$$P_{TC} = M_{PBS} + P_{SYN} + K_{PUE} \quad (3.4)$$

$P_{BS}$  is the power for BS antenna circuits (converters, mixers, filters),  $P_{SYS}$  is the local oscillator power, and the last term covers all UE circuit components (amplifiers, mixers, oscillators, filters).

### 3.3 .2 Evaluation of Channel Estimation Circuit Power (PCE)

The base station and user equipment both perform channel estimation, while their computational efficiency is measured through flops per watt. The system estimates channel state information one time during each coherence block. The base station uses linear algebra operations to process uplink pilot signals, which allows it to estimate user channels, but this process requires specific computational power.

$$P_{CE}^{(ul)} = \frac{B}{U} \frac{2\tau^{(dl)} m k^2}{L_{UE}} \quad (3.5)$$

Each UE estimates its pre-coded channel from a pilot ( $\tau_{ul}k$ ), and the downlink power (W) is calculated as:

$$P_{CE}^{(dl)} = \frac{B}{U} \frac{2\tau^{(dl)} k^2}{L_{UE}} \quad (3.6)$$

The over-channel estimation power is given as

$$P_{CE} = P_{CE}^{(ul)} + P_{CE}^{(dl)} \quad (3.7)$$

Adding the above equation together gives

$$P_{CE} = \frac{B}{U} \frac{2\tau^{(ul)} m k^2}{L_{BS}} + \frac{B}{U} \frac{2\tau^{(dl)} k^2}{L_{ue}} \quad (3.8)$$

### 3.3.3 Circuit Power for channel Coding and Decoding ( $P_{C/D}$ )

The base station sends K encoded data streams, and user devices decode them with finite computational effort. The uplink follows the reverse process [29]. The corresponding power consumption is relative to the number of bits processed and modeled according to[40].

$$P_{C/D} = \sum_{K=1}^K (E\{R_K^{(ul)} + R_k^{dl}\})(P_{COD} + P_{DEC}) \quad (3.9)$$

Both COD and  $P_{DEC}$  (W/bit/s) with  $R^{ul}$  and  $R^{dl}$  define uplink/downlink rates; EE is the expectation. Uplink and downlink are assumed equal but configurable.

### 3.3.4 Backhaul Circuit Power ( $P_{BH}$ )

Backhaul circuit power is the energy consumed to transmit data between the BS and the core network. It consists of a fixed part,  $P_{FIX}$ , independent of traffic, and a load-dependent part,  $P_{BH}$ , which scales with the system's sum rate and includes both uplink and downlink traffic.

$$P_{BH} = \sum_{k=1}^K (E\{R_k^{(ul)} + R_k^{(dl)}\}) P_{Bt} \quad (3.10)$$

$P_B$  is given (in Watts per bit/s).

### 3.3.5 Linear Processing Circuit Power ( $p_{LP}$ )

The BS applies precoding to generate the transmitted symbol vectors and combines to process the received symbol vectors. From[43]

$$P_{LP} = B \left(1 - \frac{(\tau^{ul} + \tau^{dl})k}{u}\right) \frac{2MK}{L_{BS}} + P_{LP-C} \text{ watt} \quad (3.11)$$

The first term represents the power for a single matrix–vector multiplication per symbol, and the second term represents the power for computing the combining/precoding matrices once per coherence block. If  $G = V$ , only one matrix is needed, reducing complexity. With ZF processing, this results in the corresponding computational power consumption.

$$P_{LP-C}^{(ZF)} = \frac{B}{U} \left( \frac{K3}{3L_{BS}} + \frac{3MK^2 + MK}{L_{BS}} \right) \quad (3.12)$$

## 3.4 Achievable Sum Rate

The achievable sum rate is a key performance metric that defines the maximum reliable data transmission rate of a communication system. Based on Shannon's theorem, this section evaluates the sum rate of a Massive MIMO system using Zero-Forcing (ZF) precoding with equal downlink power allocation, where channel capacity represents the data rate limit. And given as

$$R = \log_2(\mathbf{1} + SNR) \text{ bits / s / Hz} \quad (3.13)$$

SNR measures the ratio of signal to noise. Multiple data streams are transmitted simultaneously with CSI, which the transmitter obtains via feedback from all receivers. In a single-cell downlink Massive MIMO system, users can achieve their maximum data rate, given by:

$$R_k = \log_2(\mathbf{1} + SNR_k) \quad (3.14)$$

The equation below shows the achievable sum rate for k users.

$$R_{sum} = \log_2(\mathbf{1} + SNR_k) \quad (3.15)$$

With a ZF detector and  $M \geq K+1$ , the gross rate is given by:

$$R^- = B \log_2(\mathbf{1} + (m-k)) \quad (3.16)$$

ZF detection/pre-coding is applied under imperfect CSI, the average gross rate

$$R^- = B \log \left( \mathbf{1} + \frac{P^{m-k}}{\mathbf{1} + \frac{\mathbf{1}}{\tau^{ul}} + \frac{\mathbf{1}}{pk\tau^{ul}}} \right) \quad (3.17)$$

Where B stands for bandwidth.

### 3.5 Maximizing Energy Efficiency in Massive MIMO Using ZF Processing

This section presents a theoretical framework for analyzing energy efficiency (EE) in Massive MIMO systems using zero-forcing (ZF) processing. Applying ZF in both uplink and downlink makes the EE problem analytically tractable. This approach is appealing not only because it simplifies the mathematics, but also because the resulting numerical solutions are very close to the true optimal performance. According to (Eq. 3.1 for zf precoding the total EE is given as:

$$EE^{ZF} = \frac{K \left( \mathbf{1} - \frac{\tau_{Total} k}{u} \right) R}{\frac{B\alpha^2 P S_X}{\eta} + P_{CP}^{ZF}} \quad (3.18)$$

$\tau_{total} = \tau_{ul} + \tau_{dl}$ ; from (2.28), and noting that:

$$E\{R_K^{(ul)}\} + E\{R_K^{(dl)}\} = R_K^{(ul)} + R_K^{(dl)} = \left( \mathbf{1} - \frac{\tau_{total}k}{u} \right) \quad (3.19)$$

In addition

$$p_{cp}^{(ZF)} = p_{FIX} + p_{\tau c} + p_{CE} + p_{C/D} + p_{BH} + p_{LP}^{(ZF)} \quad (3.20)$$

After replacing  $p_{LP-C}$  with  $p_{LP-C}^{(ZF)}$ .

$\mathcal{A}$ ,  $\{C_i\}$ , and  $\{D_i\}$  are the constant coefficients are expressed. These coefficients are used to rewrite  $p_{LP}^{(ZF)}$  in simplified form.

$$p_{cp}^{(ZF)} = \sum_{i=0}^3 C_i K^i + M \sum_{i=0}^2 D_i K^i + AK \left( \mathbf{1} - \frac{\tau_{total}k}{u} \right) R^- \quad (3.21)$$

by considering  $\bar{R}$  and  $(M, K, R)$  putting in (3.12)

$$EE^{(ZF)} = \frac{k \left( \mathbf{1} - \frac{\tau_{Total}k}{u} \right) R^-}{B\alpha^2 pS_x + \sum_0^3 C_i k^i + M \sum_{i=0}^2 D_i k^i + AK \left( \mathbf{1} - \frac{\tau_{Total}k}{u} \right) R^-} \quad (3.22)$$

The goal is to express this equation using its parameters to maximize energy efficiency with zero-forcing precoding. First, the impact of each parameter is analyzed individually, and then the optimal values are combined to design an energy-efficient network.

Table 2: Definition of Power Consumption Coefficient

Category	Coefficients $\{C_i\}$	Expression
$\{C_i\}$	$C_1$	$P_{UE}$
$\{C_i\}$	$C_0$	$P_{FIX} + P_{SYN}$
$\{C_i\}$	$C_2$	$4B \tau^{(dl)} / (UL_{UE})$
$\{C_i\}$	$C_3$	$B / (3 L_{BS})$
$\{A_i\}$	$A$	$P_{COD} + P_{DEC} + P_{BT}$
$\{D_i\}$	$D_0$	$P_{BS}$
$\{D_i\}$	$D_1$	$B/L_{BS} (2 + 1/U)$
$\{D_i\}$	$D_2$	$B/BL_{BS} (3 - 2\tau^{(dl)})$

### 3.6 Energy Efficiency optimization with Dinkel Bach algorithm in Massive MIMO for 5G ultra-dense networks

The Dinkel Bach algorithm is widely used to optimize and maximize the energy efficiency (EE) in 5G ultra-dense networks with Massive MIMO, because EE maximization problems are typically formulated as fractional programming (FP) problems. The algorithm provides an efficient iterative method to find the optimal solution by transforming the complex non-convex fractional problem into a series of more manageable non-fractional sub-problems.

The primary function of the Dinkel Bach algorithm in this context is to handle the objective function, which is the ratio of the total achievable data rate (bits/s) to the total power consumption (Watts). EE is measured in bits/Joule.

#### Steps of Dinkel Bach's Algorithm

Initialization:  $\lambda^0 = \mathbf{0}$

1. solve  $x^t = \arg \max_x (f(x) - \lambda^t(g(x)))$
2. update  $\lambda^{(t+1)} = \frac{f(x^{(t)})}{g(x^{(t)})}$
3. Stop if:  $f(x^{(t)}) - \lambda^{(t)}g(x^{(t)}) < \epsilon$  where  $\epsilon$  is a small positive number or accuracy threshold.

In Massive MIMO: EE

$$\max_{p,m,k} \frac{\sum_k R_k(p,m,k)}{P_{total}(p,m,k)} \quad (3.23)$$

General fractional program,  $\max_{x \in X} \frac{f(x)}{g(x)}$ ,

Applying Dinkel Bach to Massive MIMO EE

$$\max_p \frac{K \log_2(\mathbf{1} + SINR(p))}{\frac{Kp}{\eta} + MP_{RF} + P_{BB} + P_0} \quad (3.24)$$

Then, applying Dinkel Bach subproblem  $\max_p K \log_2(\mathbf{1} + SINR(p)) - \lambda \left( \frac{kp}{\eta} + MP_{RF} + P_{BB} + P_0 \right)$

In energy efficiency,  $f(x)$  = total rate (bits/s),  $g(x)$  = total consumed power (W), and  $x$  are resource variables (powers, antenna counts, scheduling).

Defining the optimal fractional

$$\lambda^* = \max_{x \in X} \frac{f(x)}{g(x)} \quad (3.25)$$

Dinkel Bach transform (parametric subtractive problem). For any scalar  $\lambda \geq 0$ , define the parametric objective.

$$\Phi_\lambda = \max_{x \in X} \{f(x) - \lambda g(x)\} \quad (3.26)$$

$\Phi(\lambda) \in \mathbb{R}$  is the optimal value of a (usually simpler) optimization problem, and  $\Phi(\lambda)$  is continuous in  $\lambda$  and strictly decreasing if  $g(x) > 0$ .

From the Equivalence theorem,  $\lambda^* = 0$  and  $\lambda^*$  is the unique  $\lambda$  such that  $\Phi_\lambda = \max_{x \in X} \{f(x) - \lambda g(x)\}$

Let achieve the fractional optimum.

$$\lambda^* = \frac{f(x^*)}{g(x^*)} \quad (3.27)$$

$$f(x^*) - \lambda^* g(x^*) = 0 \quad (3.28)$$

Dinkel Bach iterative algorithm, Initialize  $\lambda^{(0)} \geq 0$  (commonly 0). For  $t=0,1,2, \dots$

$$x^{(t)} \in \arg_x \{f(x) - \lambda^{(t)} g(x), \Phi^{(t)} = f(x^{(t)}) - \lambda^{(t)} g(x^{(t)})\} \quad (3.29)$$

$$\lambda^{t+1} = f(x^{(t)}) \frac{f(x^{(t)})}{g(x^{(t)})} \quad (3.30)$$

Derivation for vector per-user power allocation (concave inner problem), model for each user  $k$ ,  $\gamma_k = a_k p_k, a_k > 0$

Under ZF approximation

$$K = (M - K) \beta_k / \sigma^2 \quad (3.31)$$

$$R(p) = B \sum_{k=1}^K \log_2(1 + a_k p_k) \quad (3.32)$$

Power consumption:

$$P_{\text{cos}}(p) = \frac{\sum_{k=1}^K p_k}{\eta} + P_{(\text{fixed})} \quad (3.33)$$

$$p_k(\lambda) = \frac{\mathbf{1}}{a_k} \left( \frac{B\eta}{\lambda \ln 2} - \mathbf{1} \right) \quad (3.34)$$

Apply non negativity:

$$p_k(\lambda) = \left[ \frac{\mathbf{1}}{a_k} \left( \frac{B\eta}{\lambda \ln 2} - \mathbf{1} \right) \right]_+ \quad (3.35)$$

where  $[z]_+ = \max\{0, z\}$ .

Derivation of stationarity for scalar transmit-power (Massive MIMO simplified model) Consider scalar optimization with decision variable  $P \in [0, P_{\text{max}}]$  Use the simplified ZF model: uniform per-user power  $p = P/K$ , identical large-scale gains  $\beta$ .

$$s(p) = \frac{p}{k} \cdot \frac{(m-k)\beta}{\sigma^2} \quad (3.36)$$

Sum rate:

$$R(p) = Bk \log_2(\mathbf{1} + s(p)) \quad (3.37)$$

Total consumed power,

$$P_{\text{cons}(P)} = \frac{P}{\eta} + P_{(\text{fixed})}, P_{(\text{fixed})} = MP_{BS} + KP_{UE} + P_O \quad (3.38)$$

Inner objective for a given  $\lambda$ ,

$$\Psi(P) = R(P) - \lambda P_{\text{cons}}(P) \quad (3.39)$$

$$P^*(\lambda) = K \cdot \frac{\mathbf{1}}{(M-K)\beta} \left( \frac{B(M-K)\beta\eta}{\lambda \ln 2} - \sigma^2 \right) \quad (3.40)$$

$$P^*(\lambda) = K \left( \frac{B\eta}{\lambda \ln 2} - \frac{\sigma^2}{(M-K)\beta} \right) \quad (3.41)$$

The analysis demonstrated that the EE optimization problem:  $EE(p) = R(p) / P(p)$  can be reformulated using a parameter  $\lambda$  and iteratively solved by maximizing  $(p, \lambda) = R(p) - \lambda P(p)$ , with  $\lambda$  updated as  $\lambda = R(p^*) / P(p^*)$  until convergence. This ensures that the final solution satisfies the optimality condition  $R(p^*) - \lambda^* P(p^*) = 0$ , confirming that the algorithm has reached the maximum achievable energy efficiency.

### 3.5.1 Energy efficiency optimization and the influence of multiple active users

In Massive MIMO, the number of active users  $K$  is determined by the base station antennas, transmit power, and target energy efficiency. Assuming fixed SINR and PA power, and a constant antenna-to-user ratio  $K=p^{-\beta}$  with  $\beta > 1$ , the system's gross rate remains constant.

$$c = (\mathbf{1} + \rho(\beta - \mathbf{1})) \quad (3.42)$$

Assuming  $\mathcal{A}$ ,  $\{C_i\}$ , and  $\{D_i\}$  are constant and non-negative, and for fixed  $p$  and  $\beta$  with a constant gross rate, the optimal number of UEs that maximizes energy efficiency (EE) can be determined accordingly [6,11,20,26].

$$k^* = \max_l [k_l^{(0)}] \quad (3.43)$$

$[k_l^{(0)}]$  denotes the real positive roots of the quadratic equation of

$$k^4 = \frac{u}{\tau_{Total}} k^3 - \mu_1 k^2 - \mu_0 k \frac{u \mu_0}{\tau_{Total}} = \mathbf{0} \quad (3.44)$$

$$\mu_0 = \frac{\frac{u}{\tau_{Total}} (c_1 + \beta^{-1} D_1) (c_1 + \beta^{-1} D_1)}{C_2 + B D_2} \quad (3.45)$$

The optimal  $K^*$  is the integer closest to the quadratic root that maximizes energy efficiency.

Although quartic equations have closed-form solutions, practical numerical methods are simpler and more accurate. For parameter analysis, linear processing and channel estimation power are neglected, which is reasonable under high computational efficiencies  $L_{Bs}$  and  $L_{UE}$

$$k^* = \left[ \mu \left( 1 + \frac{u}{u_{\text{total}} \mu} \right) \right] \quad (3.46)$$

$$\mu = \frac{c_o + \frac{B\alpha^2 p S_x p^-}{\eta}}{c_{1+\beta D_o}} = \frac{P_{\text{FIX}} + P_{\text{SYS}} + \frac{B\alpha^2 P S_x P^-}{\eta}}{P_{\text{UE}} + \beta^- P_{\text{BS}}} \quad (3.47)$$

From (3.26)– (3.27), the optimal  $K^*$  decreases with power terms independent of  $K$  and  $M$ , but increases with PA power, noise power, and cell radius, meaning more UEs should be served in larger coverage areas. When linear processing and channel estimation power are negligible,  $K^*$  decreases with UE/BS hardware power, is unaffected by rate-dependent power, and increases with fixed system power.

### 3.5.2 Energy efficiency optimization and the influence of multiple active antennas

When the BS antenna is greater than  $k$  users, EE in (3.7) increases. For fixed numbers of active users and transmit power, the BS antenna count that maximizes EE can be determined [9].

$$M^{(+)} = \frac{e^{\left( \frac{p(B\alpha^2 p S_x P + c)}{D_1 e} \right) + p \frac{k-1}{e}} + 1}{P} pK - 1 \quad (3.48)$$

where the constants  $C' > 0$  and  $D' > 0$  are defined as

$$C' = \frac{\sum_{i=0}^3 c_i k^i}{k} \quad \text{and} \quad D' = \frac{\sum_{i=0}^3 D_i k^i}{k} \quad (3.49)$$

This expression determines the optimal antenna number  $M$  that maximizes EE in Massive MIMO. The optimal  $M^*$  is independent of rate-dependent power, decreases with higher BS antenna power  $P_{\text{BS}}$ , and increases with fixed and UE-dependent powers ( $P_{\text{FIX}}$ ,  $P_{\text{SYS}}$  and  $P_{\text{UE}}$ ). Moreover,  $M^*$  grows nearly linearly with  $S_x$  and thus with cell radius  $d_{\text{max}}$  and the number of users  $K$ .

### 3.5.3 Energy efficiency optimization and the influence of transmit power

Since transmit power scales with SNR, maximizing energy efficiency under ZF processing requires jointly optimizing  $M$  and  $K$ ; for given values, the EE-optimal transmit power  $p \geq 0$  can then be computed accordingly.

$$p^* = \frac{e^{\left( \frac{\eta (m-k)(C'+MD')}{\beta \eta^2 p s_x e} \right) - 1}}{m - k} \quad (3.50)$$

The optimal transmit power  $p^*$  increases with  $C'$  and  $D'$ , and thus with the circuit power coefficients. Under ZF processing, this corresponds to the transmit power that maximizes the total PA power

$$P_{TX}^{(ZF)} = \frac{\beta \partial^2 p s_x}{\eta} KP^* \quad (3.51)$$

The optimal transmit power is independent of rate-dependent power ( $P_{COD}$ ,  $P_{DEC}$ ,  $P_{BT}$ ) but increases with fixed and per-antenna power ( $P_{BS}$ ,  $P_{FIX}$ ,  $P_{SYS}$ ,  $P_{UEP}$ ). This makes sense because when fixed-circuit power is large, higher PA power has little impact on total consumption, allowing higher rates.

It has shown in [43] and [42] In TDD systems, power can scale down with  $1/M$  (perfect CSI) or  $1/\sqrt{m}$  (imperfect CSI) while maintaining rates, but this is not energy-optimal. Maximum EE is achieved by increasing power with  $M$ .

### 3.5.4 Energy efficiency optimization and the influence of throughput

Massive MIMO boosts area throughput and lowers per-antenna power by serving many UEs via spatial multiplexing. Throughput gains from extra RF chains and SDMA processing increase circuit power, so EE is maximized by balancing these factors. Using random-matrix theory, for large  $M$  and  $K$  with finite  $M/K$ , the asymptotic data rate yields a closed-form EE expression for optimization. By random matrix theory [19], it converges in mean square to the average rate; thus, the asymptotic rate can be used as the average.

## CHAPTER FOUR

### SIMULATION AND RESULTS DISCUSSION

#### 4.1 Introduction

MATLAB is used for simulations. Simulations of the major design parameters are done with the aim of evaluating their impact on the optimization of energy efficiency, as presented under perfect and imperfect channel state information. The optimal design parameters for maximizing energy efficiency are obtained through simulations using the Dinkel Bach algorithm with ZF processing. A sample Massive MIMO setup is considered with 200 antennas, 80 active users, and a 20 MHz bandwidth, and the corresponding simulation parameters are summarized in the table below.

#### 4.2 Simulation parameters

The MATLAB demonstration uses the specified parameters to illustrate system performance. These values are mainly derived from standard reports of the International Telecommunication Union and established reference values. [[43], [34] [38][45][17][46].

Table 3 Simulation parameters

Parameter	Symbol	Value
Carrier frequency	$F_c$	2 GHz
Cell radius (single-cell)	$D_{max}$	250 m
Minimum distance	$D_{min}$	35 m
Channel coherence bandwidth	$B_C$	180 kHz
Channel coherence time	$T_C$	10 ms
Coherence block (symbols)	$U$	1800
Computational efficiency at BSs	$L_{BS}$	10 Gops/w
Computational efficiency at UEs: $L_{UE}$	$L_{UE}$	5 Gop/W
Fixed power consumption	$P_{FIX}$	18 W
Fraction of downlink transmission	$\zeta_{dl}$	0.6

Fraction of uplink transmission	$\zeta(\text{ul})$	0.4
PA efficiency at UEs	$\eta(\text{ul})$	0.3
PA efficiency at BSs	$\eta(\text{dl})$	0.39
Local oscillator power at BS	$P_{\text{SYN}}$	2 W
Backhaul power	$P_{\text{BT}}$	0.25 W/(Gbit/s)
Coding power	$P_{\text{COD}}$	0.1 W/(Gbit/s)
Decoding power	$P_{\text{DEC}}$	0.8 W/(Gbit/s)
Circuit power at BS	$P_{\text{BS}}$	1 W
Circuit power at UE	$P_{\text{UE}}$	0.1 W
Pilot lengths (UL/DL)	$\tau(\text{ul}), \tau(\text{dl})$	1
Total noise power	$B\sigma^2$	101 dBm
Transmission bandwidth	$B$	20 MHz

### 4.3 Simulation and result discussion

#### 4.3.1 Impact of the number of massive base station antennas on energy efficiency optimization

Figure 4.1 shows how energy efficiency (EE) varies with the number of base station antennas ( $M$ ). It compares Zero-Forcing (ZF) and Dinkel Bach-based EE optimization under both perfect and imperfect channel state information (CSI) conditions.

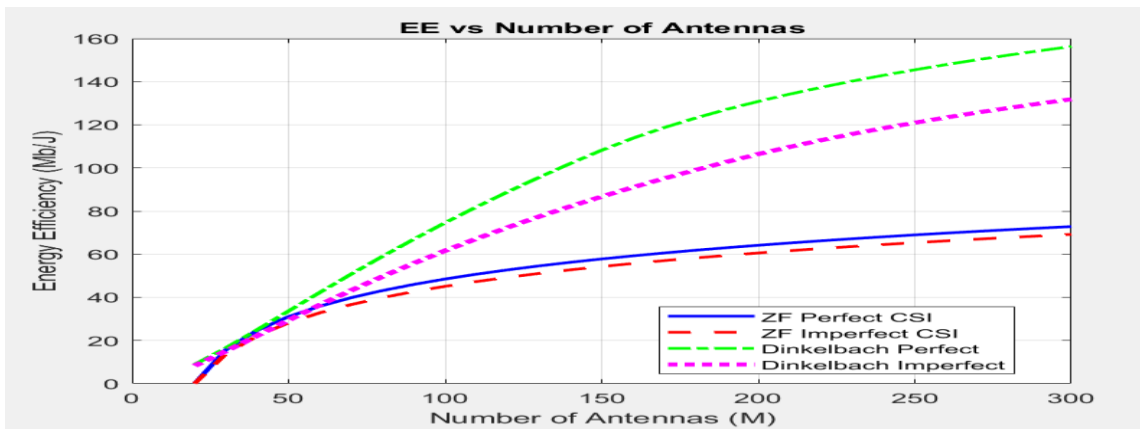


Figure 4.1 simulation of EEvs antenna

Figure 4.1 depicts the EE scaling characteristics with the number of base station antennas in the context of the massive MIMO system with zero-forcing, where conventional zero-forcing is compared with Dinkel Bach-based EE optimization, considering both channel conditions

The EE is seen to scale with the number of base station antennas in all cases, owing to improved array gain and interference cancellation, thereby increasing the data rates without an accompanying increase in power consumption. The conventional zero-forcing method, however, is seen to experience diminishing EE benefits with an increasing number of base station antennas, owing to the increasing cost of circuit power and processing power, which dominate the benefits of beamforming.

On the other hand, the zero-forcing method, which is optimized via the Dinkel Bach approach, is seen to achieve superior EE benefits across the entire range of base station antenna counts. The CSI is also seen to have a significant impact on the EE benefits, where perfect CSI is seen to achieve superior EE benefits, while imperfect CSI is seen to result in reduced SINR owing to imperfect interference cancellation. Nevertheless, the Dinkelbach approach is seen to achieve superior EE benefits compared with conventional zero-forcing, even in the context of imperfect CSI.

Thus, Figure 4.1 is seen to confirm the effectiveness of large antenna arrays in improving EE benefits, where the Dinkel Bach approach is seen to be particularly effective in the context of massive MIMO systems.

Table 4. Energy Efficiency (Mb/J) vs Number of Antennas

Number of base station Antennas	ZF Perfect CSI	ZF Imperfect CSI	Dinkel Bach Perfect	Dinkel Bach Imperfect
50	29	28	34	33
100	48.5	45	102	72
150	58	54	108	87
200	64	60	130	106

### 4.3. 2.Impact of the number of active users on energy efficiency optimization

The graph presented in Figure 4.2 shows the change in energy efficiency (EE) with the user number (K) in a Massive MIMO system that uses Zero-Forcing (ZF) for pre-coding. This change is demonstrated for both perfect and imperfect channel state information (CSI) scenarios. Dinkel Bach-based energy efficiency optimization is compared with the conventional ZF method regarding the performance achieved. In regions of few users, the energy efficiency of all curves increases rather steeply with the number of users.

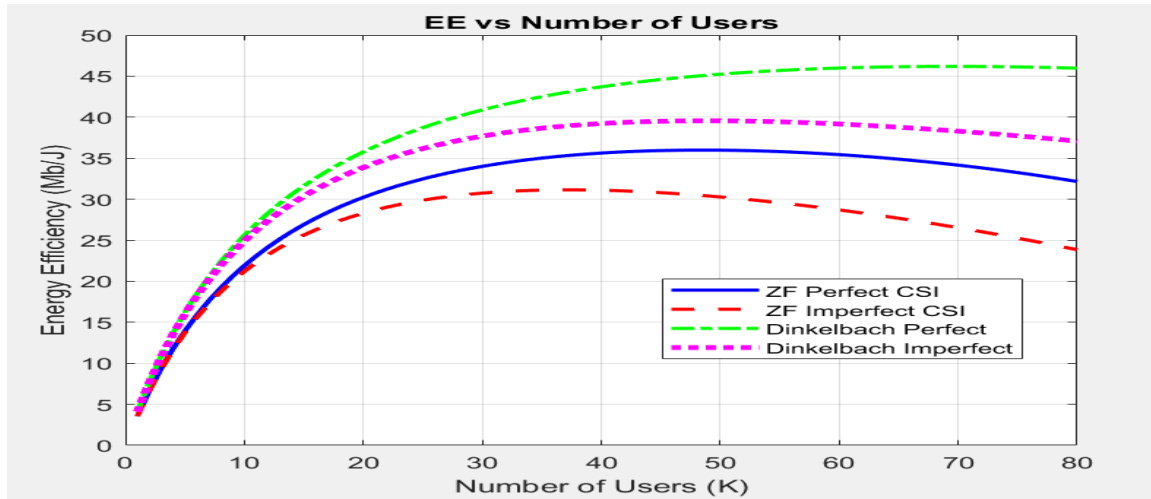


Figure 4.2 Simulation of EEvs user

As depicted in the figure *above*, EE increases with the number of supported users at the beginning due to the increased multiuser multiplexing gains. Supporting more users considerably increases the sum rate, whereas the power increase is relatively smaller, resulting in the rapid increase of the EE. After the optimal number of users, EE decreases. Supporting more users not only increases the power of the circuit, backhaul, and signal processing but also increases the pilot power and the residual multiuser interference. Therefore, the increment of the sum rate is not sufficient to compensate the increased power, resulting in the decreased EE.

Perfect CSI always has higher EE compared to the case of imperfect CSI. Imperfect CSI causes interference due to channel estimation errors, leading to the degradation of the SINR and the sum rate, resulting in the degradation of the EE.

For all the operating regions, the Dinkelbach method-based ZF has higher EE compared to the conventional ZF method. Energy-aware fractional programming indeed provides more efficient Massive MIMO system performance, whereas the imperfections of the CSI considerably limit the achievable EE gains.

Table 5 Energy Efficiency (Mb/J) vs Number of Users

Number of Users (K)	ZF Perfect CSI	ZF Imperfect CSI	Dinkel Bach Perfect	Dinkel Bach Imperfect
5	13.73	13.73	16.2	16
10	22	21	25.6	25
20	30	28	35	33
30	31	34	41	38
40	36	31	44	39
50	36	30	45.5	40
60	35	28.69	46	39.16
70	34.15	26.25	46	38.29
80	32.154	23.84	45.9676	37.0774

### 4.3.3 The impact of system throughput on energy efficiency optimization

Figure 4.3. shows the trade-off between energy efficiency (EE) and throughput for a massive MIMO system using ZF pre-coding with fixed transmit power and Dinkel Bach-based power optimization. As throughput increases, EE decreases for both schemes due to the higher transmit power required to achieve larger data rates.

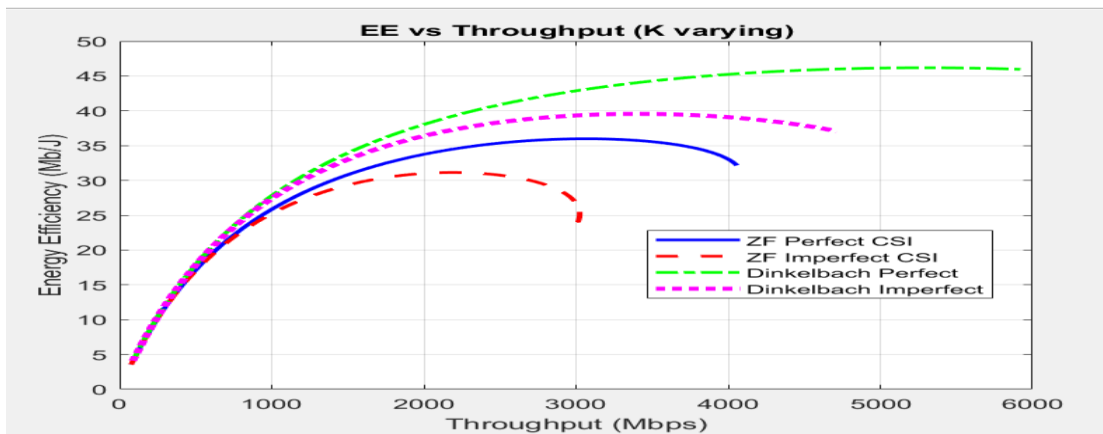


Figure 4.3 Simulation of EEvs throughput( varying k)

The throughput varied by adjusting the number of active users. All the curves show a quasi-concave pattern, with initially rising to the highest point and then slowly declining. The figures illustrate the very trade-off situation between the two properties, energy efficiency, and throughput. A trio of low throughput, increasing data rate has turned out to be the best instance for EE as the rate wins over the power consumption related to that. After the optimum operating point, the enhancement of throughput demands excessively more power than the signal and circuit together, thus leading to lower EE. The effect of the quality of CSI is very clear, as the systems with perfect CSI always get more EE than those with imperfect CSI. Errors in channel estimation in the case of imperfect CSI cause residual interference, which in turn reduces the maximum. Overall, the figure confirms the existence of an optimal throughput region for energy-efficient operation and emphasizes that energy-aware optimization is essential to sustain high EE in high-throughput Massive MIMO systems. Data rate for a given power budget and then causes faster EE degradation at higher throughput levels.

Table 6 Energy Efficiency (Mb/J) vs Throughput (Mbps)

Throughput (Mbps)	ZF Perfect CSI EE (Mb/J)	ZF Imperfect CSI EE (Mb/J)	DinkelBach Perfect EE (Mb/J)	DinkelbachImperfect EE (Mb/J)
200	5	5	5	5
500	15	14	16	15
1000	25	24	28	27
1500	31	29	34	32
2000	34	31	38	36
2500	35.5	31	41	38.5
3000	36	25	42	39
3500	35	—	45	39
4000	32.5	—	46	38
5000	—	—	46.5	—
6000	—	—	46	—

(“—” means that the curve does not extend to that throughput in the plot.)

#### 4.3.4 Impact of transmit power on energy efficiency optimization.

This figure presents the variation of Energy Efficiency (EE, in Mb/J) with respect to the transmit power per user (in Watts) for two pre-coding schemes, ZF and the Dinkel Bach optimization algorithm under both perfect and imperfect CSI.

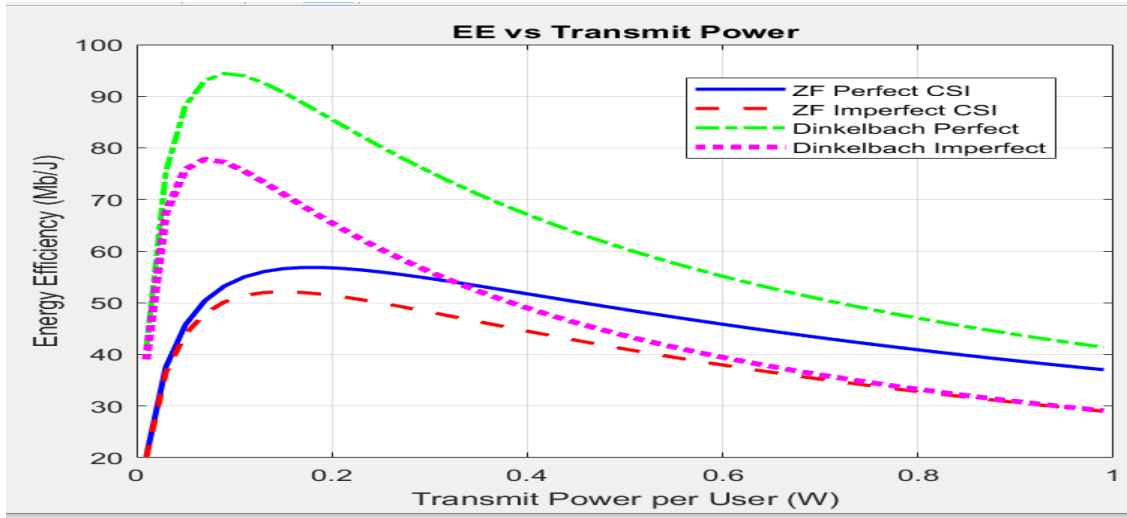


Figure 4.4 Simulation of EEvs transmit power

Massive MIMO systems utilizing Zero-Forcing (ZF) precoding, along with the Dinkel Bach-based energy efficiency optimization for both perfect and imperfect channel state information (CSI), are shown in Figure 4.4 to have the energy efficiency (EE) varying with the transmit power per user. EE reveals a quasi-concave relationship with power for all proposed methods. At low power levels, a rise in the transmit power results in a substantial increase of the EE because the data rate becomes the major contributor to total power consumption. But increasing the power further from the optimal level causes the EE to decrease since the additional power no longer compensates for the much higher power consumption in the power amplifier and circuitry especially when it comes to the total power.

Dinkel Bach-based optimization is a lot better than the conventional ZF over the full range of transmit power. It is able to get the highest peak EE at a smaller transmit power, indicating better energy usage and a more efficient power distribution. Also, the gap in the performance of the perfect and imperfect cases is reduced for the Dinkel Bach method, which is a sign of improved tolerance to CSI imperfections compared to ZF pre-coding. All in all, the illustration reveals a certain transmit power level that is the same as the one that maximizes energy efficiency, and it also confirms that an

increase in transmit power alone does not result in better EE. The Dinkel Bach algorithm is best for the optimization techniques that are a must for the promotion of sustainable and efficient operation in Massive MIMO systems.

Table 7 Energy Efficiency (Mb/J) vs Transmit Power per User (W)

Transmit Power (W)	ZF Perfect CSI	ZF imperfect CSI	DinkelBach Perfect	DinkelBach imperfect EE (Mb/J)
	EE (Mb/J)	EE (Mb/J)	EE (Mb/J)	
0.02	28	25	70	65
0.05	45	42	90	75
0.10	54	50	94	78
0.20	57	52	85	65
0.40	52	45	68	50
0.60	47	40	57	40
0.80	42	35	48	34
1.00	38	30	42	30

#### 4.3.5 The impact of cell density on energy efficiency optimization

Figure 4.5 shows how energy efficiency (EE) changes with cell density (cells/km<sup>2</sup>), different system configurations being considered, such as SISO, SIMO, MIMO, Massive MIMO with ZF pre-coding under imperfect CSI, and the proposed Dinkel Bach-based energy efficiency optimization under both perfect and imperfect CSI. It was noted that for all the schemes, energy efficiency got lower with the increase in cell density

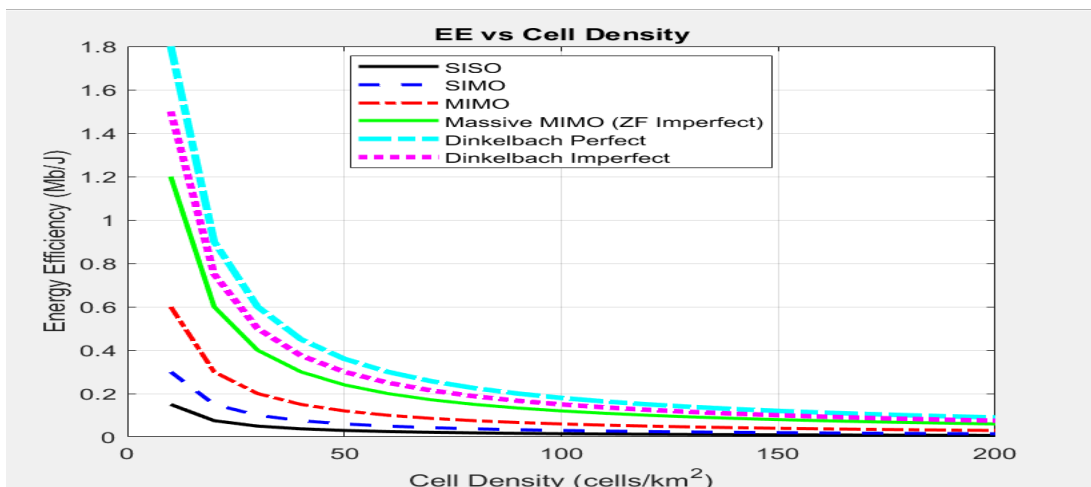


Figure 4.5 Simulation of EEvs cell density

The high EE at lower cell densities was mainly due to the above-mentioned factors like bigger cell coverage, lower inter-cell interference, and less signaling and coordination overhead. With an increase in cell density, the higher the number of base stations, the more power consumed for circuits, backhaul, and signaling, not to mention the even bigger inter-cell interference that degrades energy efficiency. Of all the baseline systems, SISO has the least EE, followed by SIMO and conventional MIMO, which points to the limited spatial gains of low-dimensional antenna systems. Massive MIMO with ZF precoding gets a lot more EE than conventional MIMO due to the better beam forming and spatial multiplexing gains, even under imperfect CSI. The Dinkel Bach-based optimization has the best energy efficiency at all cell densities. It places the upper bound on EE performance in the perfect CSI case, while the imperfect CSI case is still above the level of Massive MIMO with ZF pre-coding. This proves the usefulness of energy-aware optimization in reducing power consumption and interference problems that come with network densification. The EE curves for all methods come together slowly at higher cell densities, which means that there is less and less energy gain from further densification. This whole saturation behavior points to the fact that beyond a certain density, extra infrastructure and operational energy costs turn out to be more than the throughput gains that can be achieved. The overall depicted scenario makes it clear that the energy efficiency has been improved by means of high-tech antenna systems and densification, but the benefits, in fact, are not realized until they are combined with smart, energy-efficient optimization strategies like the Dinkel Bach algorithm. This underlines the need for network architecture and optimization algorithms to be designed together in order to realize the vision of eco-friendly cellular networks.

Table8. Simulation result of EE vs cell density

Cell Density (cells/km <sup>2</sup> )	SISO EE (Mb/J)	SIMO EE (Mb/J)	MIMO EE (Mb/J)	Massive MIMO (ZF Imperfect)	Dinkelbach Perfect EE (Mb/J)	Dinkelbach Imperfect (Optimized) EE (Mb/J)
10	0.15	0.3	0.6	1.2	1.8	1.5
20	0.075	0.15	0.3	0.6	0.9	0.75
50	0.03	0.06	0.12	0.24	0.36	0.3
100	0.015	0.03	0.06	0.12	0.18	0.15
150	0.01	0.02	0.04	0.08	0.12	0.1
200	0.0075	0.015	0.03	0.06	0.09	0.075

#### 4.3.6 The relationship between energy efficiency and spectra efficiency

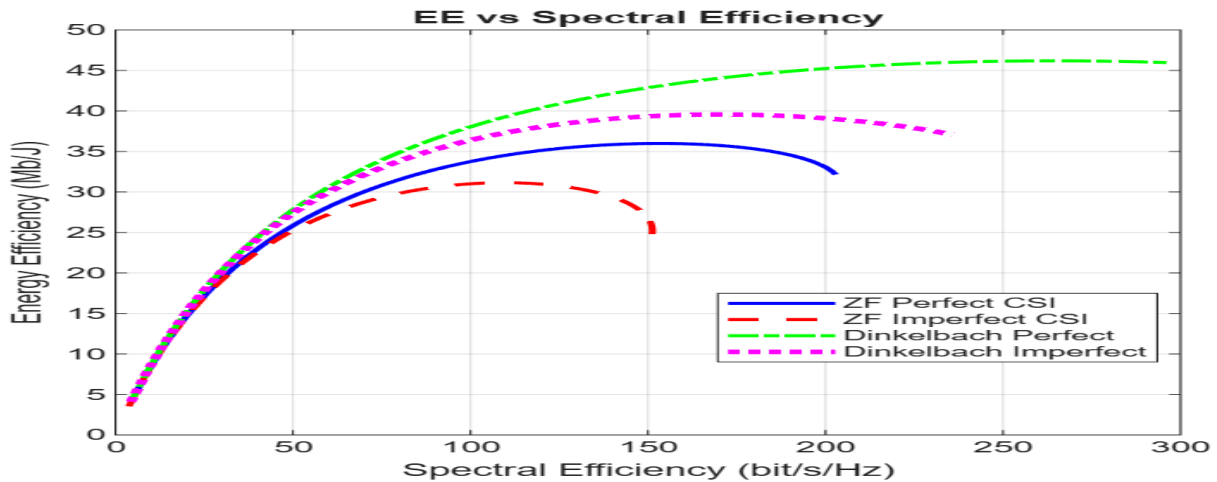


Figure 4.6 EEvs SE

Figure 4.6 displays the relation between energy efficiency versus spectral efficiency for ZF and Dinkel Bach-based schemes with both perfect and imperfect CSI. In all cases, the energy efficiency increases with spectral efficiency for low values of spectral efficiency due to better utilization of radio resources. However, it decreases beyond a certain value since higher spectral efficiencies need significantly more transmit and circuit power to achieve. This confirms the fundamental energy efficiency-spectral efficiency trade-off in a massive MIMO system. The perfect CSI curves

outperform those with imperfect CSI in all regions. This quantifies the performance loss because of channel estimation errors. In addition, the maximum energy efficiency is higher for Dinkel Bach-optimized schemes, and they offer better performance over a wider range of spectral efficiencies, which explains the effectiveness of optimization in improving energy-efficient operation.

Table.9 Simulation result of EE vs SE

Method	CSI Condition	Spectral Efficiency (bits/s/Hz)	Energy Efficiency (Mb/J)
ZF	Perfect CSI	150	36
ZF	Imperfect CSI	120	31
Dinkel Bach	Perfect CSI	260	46
Dinkelbach	Imperfect CSI	165	39.5

### 4.3.7 The relationship between energy efficiency and data rate

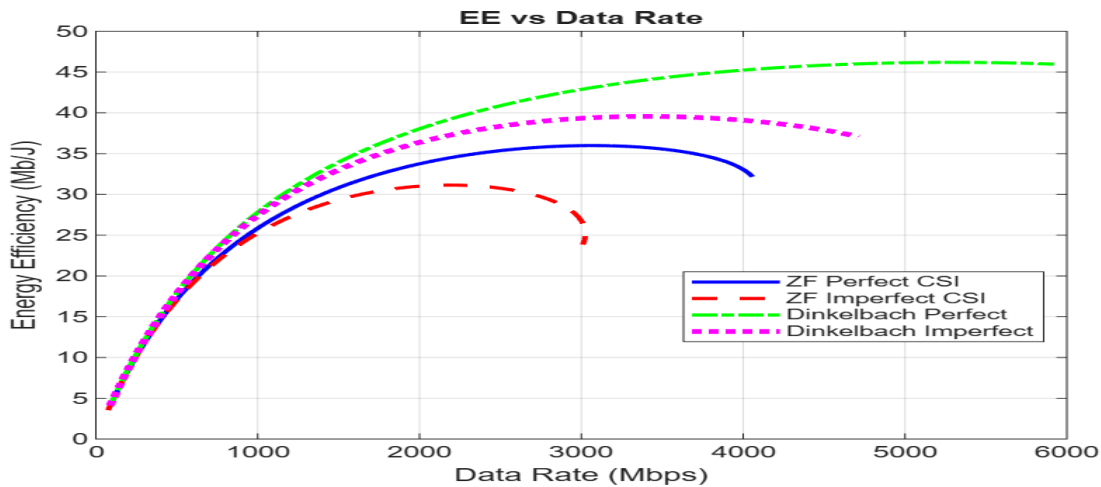


Figure 4.7 EE VS data rate

As presented in Figure 4.7, in a massive MIMO system with a typical zero-forcing method and a Dinkel Bach-based optimization approach with ideal and non-ideal CSI, there exists a rapid increase in energy efficiency with respect to the data rate, peaking at a certain data rate and falling gradually with a large data rate, as more energy becomes required. Also, schemes that use the Dinkel Bach method always provide a higher EE and a greater energy-efficient operation compared to traditional

ZF schemes, verifying effectiveness in the context of optimizing the fractional energy efficiency. Besides, when there is a perfect CSI, a greater EE will be offered compared to when there is an imperfect CSI, because there will be an increase in power consumption as well as a reduction in achievable rates.

Table. 10. EE VS data rate

Method	CSI Condition	Data Rate (Mbps)	Energy Efficiency (Mb/J)
ZF	Perfect CSI	3000	36
ZF	Imperfect CSI	2200	31
Dinkel Bach	Perfect CSI	5200	46
Dinkel Bach	Imperfect CSI	2800	39

### 4.3.8 Optimizing energy efficiency by using Massive MIMO

Figure 4.6 provides a visualization of the three-dimensional energy efficiency (EE) surface as a joint function of the active users ( $K$ ) and the base station antennas ( $M$ ), which has been derived through the Dinkel Bach-based energy efficiency optimization algorithm

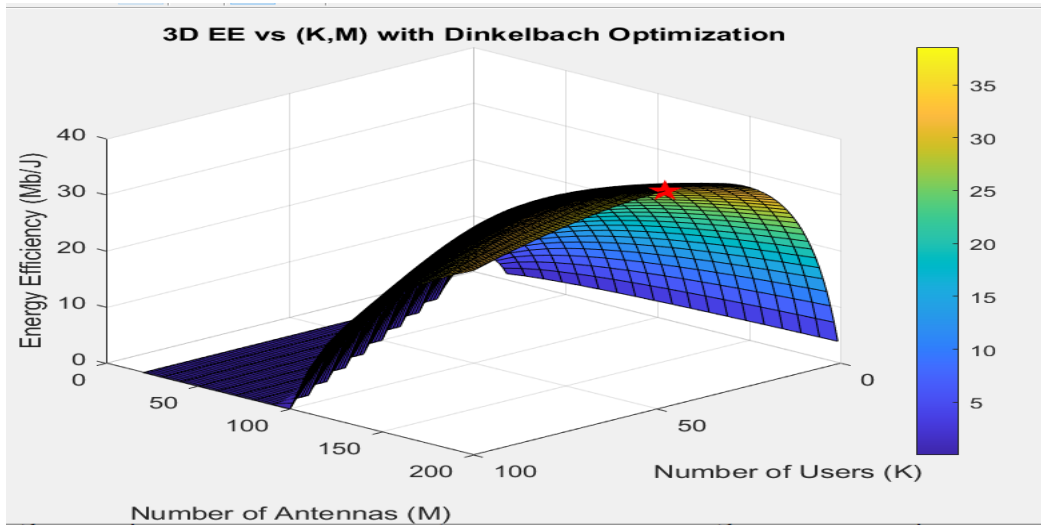


Figure 4.8 3D simulation of EEvs (K, M)

The surface has been very clearly shown that the energy efficiency will be dependent on the  $K$  and  $M$  together, and there is a single optimal operating region where EE is at its highest. If the user count is held constant, the initial increase in the number of antennas leads to a large amount of EE being gained as a result of the better techniques used in beam forming and spatial multiplexing combined. Nevertheless, the energy efficiency will reach a point where it will not increase anymore and eventually start to decline when the power used for circuits and signal processing consumes all the rate improvements that can be drawn from the antenna count. In the same way, and with the same number of antennas, the increase in the users at first leads to the power efficiency being improved as more users can be inferred from the input signal and more spatial degrees of freedom are liberated for the users. After reaching the optimal point, further increases in the user count result in even more inter-user interference, increased pilot overhead, and additional power consumption, which collectively reduce energy efficiency. The marked peak on the surface highlights the best combination of ( $K$ ,) that results in the maximum EE. This perfect place indicates that one could not

reach the energy-efficient operation just by the sole means of either of the two competing strategies, namely, maximizing the number of antennas or maximizing the number of users. Instead, it requires one to do a proper system dimensioning to achieve the best EE performance. In general, the above-mentioned figure gives an essential design perspective for Massive MIMO systems through demonstrating the non-linear and coupled aspects of system size and energy efficiency. The findings not only affirm the utility of the Dinkel Bach optimization methodology in locating the EE-optimal setup but also stress the role of simultaneous antenna–user allocation in building sustainable and energy-efficient network deployment.

#### Dinkel Bach optimization results

- Optimal K: 48, Optimal M: 200, Optimal EE: 38.56 Mb/J
- Maximum EE for ZF Perfect CSI (K varying): 35.98 Mb/J at K=48
- M Maximum EE for Dinkel Bach Perfect (K varying): 46.19 Mb/J
- Maximum EE for Dinkel Bach Imperfect (K varying): 39.56 Mb/J
- maximum EE for ZF Imperfect CSI (K varying): 31.14 Mb/J at K=37

Table 11 comparison our work with related previous work

Ref no	Year	Numbers of Bs antenna(M)	Numbers user k	Numbers throughput (Mbps)	transmit power	No of data rate (Mbps)	EE vs M	EE vs K	EE vs data rate	EE vs SE	Optimized EE vs K, M	EE vs cell density
46	2022	200	10	36-	1w	-	18	-	35	28.9	-	-
38	2020	220	80	-	1w	60	15	-	4	'	8.9	-
45	2022	100	40	-	1w	-	0.4	-	-	15		
This work	2026	200	80	3000	1w	60	105	37	39	39.5	38.56	1.5

Note (-) work that not investigated in previous

## **CHAPTER FIVE: CONCLUSION AND RECOMMENDATIONS**

### **5.1 Conclusion**

This thesis conducted a thorough simulation into the energy efficiency (EE) optimization of 5G ultra dense wireless networks by using Massive MIMO systems using MATLAB-based simulations under both perfect and imperfect channel state information (CSI) scenarios. The optimization incorporated with Zero-Forcing (ZF) pre-coding and Dinkel Bach-based energy efficiency optimization, while at the same time assessing the effect of major system parameters such as the number of base station antennas, number of active users, throughput, transmit power, and cell density upon the comparison. Simulation results conclusively show that there is an increase in energy efficiency with more antennas, user multiplexing, and cell density; however, these gains are accompanied by diminishing returns since the circuit, processing, and backhaul power consumption are also rising. There is a specific optimal operating point corresponding to the number of antennas, users, throughput, and transmit power that results in the maximum EE. Moving beyond these points results in lower efficiency even though the system capacity is higher. In all scenarios, the Dinkel Bach-based optimization was consistently superior to the traditional ZF pre-coding, and it not only reached higher peak energy efficiency but also showed greater robustness to the imperfections in the CSI. Moreover, it was indicated by the results that the presence of imperfect CSI hurts EE because of the residual interference and the requirement for additional power, but energy-aware optimization is very effective in reducing that degradation. The results in general confirm that the energy efficiency optimization of 5G ultra dense wireless networks using Massive MIMO systems is a joint optimization problem and is not an automatic effect of large-scale deployment. The Dinkel Bach algorithm, in this connection, can be regarded as an effective and scalable solution for facilitating energy-efficient operation under realistic system constraints.

## 5.2 Recommendations

This research conducts the energy efficiency optimization techniques of 5G ultra dense wireless networks using Massive MIMO incorporated with Zero-Forcing (ZF) pre-coding and Dinkel Bach-based energy efficiency optimization. It has several limitations and miss Robust Algorithms for Imperfect CSI.

Therefore, I recommend that future researchers in the following area extend their studies

1. Develop Adaptive and Robust Algorithms for Imperfect CSI: Machine learning-based channel estimation to reduce pilot overhead and improve accuracy.
2. Implement Intelligent Antenna and User Load Management
3. Integrate Multi-Layer Power Modeling in Optimization.
4. Pursue Network-Level EE Optimization
5. Hardware Algorithm Co-Design for Energy Efficiency: Exploring novel antenna architectures (e.g., hybrid beam forming, dynamic meta surface antennas) that offer better energy–performance trade-offs.

## References

- [1] V. Poirot, M. Ericson, M. Nordberg, and K. Andersson, “Energy efficient multi-connectivity algorithms for ultra-dense 5G networks,” *Wirel. Networks*, vol. 26, no. 3, pp. 2207–2222, 2020, doi: 10.1007/s11276-019-02056-w.
- [2] S. Buzzi and C. D’Andrea, “Energy Efficiency and Asymptotic Performance Evaluation of Beamforming Structures in Doubly Massive MIMO mmWave Systems,” *IEEE Trans. Green Commun. Netw.*, vol. 2, no. 2, pp. 385–396, 2018, doi: 10.1109/TGCN.2018.2800537.
- [3] H. T. S. AlRikabi, A. H. M. Alaidi, A. S. Abdalrada, and F. T. Abed, “Analysis of the efficient energy prediction for 5G wireless communication technologies,” *Int. J. Emerg. Technol. Learn.*, vol. 14, no. 8, pp. 23–37, 2019, doi: 10.3991/ijet.v14i08.10485.
- [4] D. Borges, P. Montezuma, R. Dinis, and M. Beko, “Massive mimo techniques for 5g and beyond—opportunities and challenges,” *Electron.*, vol. 10, no. 14, pp. 1–29, 2021, doi: 10.3390/electronics10141667.
- [5] T. X. Tran and K. C. Teh, “Spectral and Energy Efficiency Analysis for SLNR Precoding in Massive MIMO Systems with Imperfect CSI,” *IEEE Trans. Wirel. Commun.*, vol. 17, no. 6, pp. 4017–4027, 2018, doi: 10.1109/TWC.2018.2819184.
- [6] S. M. Nimmagadda, “Optimal spectral and energy efficiency trade-off for massive MIMO technology: analysis on modified lion and grey wolf optimization,” *Soft Comput.*, vol. 24, no. 16, pp. 12523–12539, 2020, doi: 10.1007/s00500-020-04690-5.
- [7] S. A. Busari, K. M. S. Huq, S. Mumtaz, L. Dai, and J. Rodriguez, “Millimeter-Wave Massive MIMO Communication for Future Wireless Systems: A Survey,” *IEEE Commun. Surv. Tutorials*, vol. 20, no. 2, pp. 836–869, 2018, doi: 10.1109/COMST.2017.2787460.
- [8] T. L. Marzetta and B. Labs, “Massive MIMO and Beyond,” *Inf. Theor. Perspect. 5G Syst. Beyond*, pp. 299–338, 2022, doi: 10.1017/9781108241267.009.
- [9] I. H. Ahmed and A. A. Abdulkafi, “Energy-Efficient Massive MIMO Network,” *Tikrit J. Eng. Sci.*, vol. 30, no. 3, pp. 1–8, 2023, doi: 10.25130/tjes.30.3.1.
- [10] M. A. Adedoyin and O. E. Falowo, “Combination of ultra-dense networks and other 5G enabling technologies: A survey,” *IEEE Access*, vol. 8, pp. 22893–22932, 2020, doi: 10.1109/ACCESS.2020.2969980.
- [11] K. Zheng, S. Ou, and X. Yin, “Massive MIMO channel models: A survey,” *Int. J. Antennas Propag.*, vol. 2014, 2014, doi: 10.1155/2014/848071.
- [12] S. A. Khwandah, J. P. Cosmas, P. I. Lazaridis, Z. D. Zaharis, and I. P. Chochliouros, “Massive MIMO Systems for 5G Communications,” *Wirel. Pers. Commun.*, vol. 120, no. 3, pp. 2101–2115, 2021, doi: 10.1007/s11277-021-08550-9.
- [13] E. Björnson, J. Hoydis, and L. Sanguinetti, “Massive MIMO networks: Spectral, energy, and

- hardware efficiency,” *Found. Trends Signal Process.*, vol. 11, no. 3–4, pp. 154–655, 2017, doi: 10.1561/20000000093.
- [14] L. D. Nguyen, T. Q. Duong, H. Q. Ngo, and K. Tourki, “Energy Efficiency in Cell-Free Massive MIMO with Zero-Forcing Precoding Design,” *IEEE Commun. Lett.*, vol. 21, no. 8, pp. 1871–1874, 2017, doi: 10.1109/LCOMM.2017.2694431.
- [15] J. Isabona and V. M. Srivastava, “Energy-efficient communication in large scale antenna systems: Impact of variable user capacity and number of transmission antennas,” *Prog. Electromagn. Res. M*, vol. 58, no. August, pp. 205–213, 2017, doi: 10.2528/PIERM17052306.
- [16] A. Salh *et al.*, “Energy-Efficient Low-Complexity Algorithm in 5G Massive MIMO Systems,” *Comput. Mater. Contin.*, vol. 67, no. 3, pp. 3189–3214, 2021, doi: 10.32604/cmc.2021.014746.
- [17] G. P. Tan and L. Materum, “5G Massive MIMO and its Impact on Energy Efficiency,” *Eurasia Proc. Sci. Technol. Eng. Math.*, vol. 22, pp. 87–98, 2023, doi: 10.55549/epstem.1337636.
- [18] P. R. Masadi and V. Bandi, “Design and Optimization of Massive MIMO Systems for 5G Networks,” 2024.
- [19] S. K. G. Peesapati, “Energy Efficiency of 5G Radio Access Networks,” p. 70, 2020, [Online]. Available: <http://www.diva-portal.org/smash/record.jsf?pid=diva2%3A1523762&dswid=-2686>
- [20] “Chunguang Lu a.”
- [21] R. M. Asif, J. Arshad, M. Shakir, S. M. Noman, and A. U. Rehman, “Energy Efficiency Augmentation in Massive MIMO Systems through Linear Precoding Schemes and Power Consumption Modeling,” *Wirel. Commun. Mob. Comput.*, vol. 2020, 2020, doi: 10.1155/2020/8839088.
- [22] S. Marwaha *et al.*, “Energy Efficient Operation of Adaptive Massive MIMO 5G HetNets,” *IEEE Trans. Wirel. Commun.*, vol. 23, no. 7, pp. 6889–6904, 2024, doi: 10.1109/TWC.2023.3336059.
- [23] H. Q. Ngo, G. Interdonato, E. G. Larsson, G. Caire, and J. G. Andrews, “Ultradense Cell-Free Massive MIMO for 6G: Technical Overview and Open Questions,” *Proc. IEEE*, vol. 112, no. 7, pp. 805–831, 2024, doi: 10.1109/JPROC.2024.3393514.
- [24] E. Björnson, J. Hoydis, and L. Sanguinetti, *Massive MIMO networks: Spectral, energy, and hardware efficiency*, vol. 11, no. 3–4. 2017. doi: 10.1561/20000000093.
- [25] C. Desset, B. Debaillie, and F. Louagie, “Towards a flexible and future-proof power model for cellular base stations,” *2013 24th Tyrrhenian Int. Work. Digit. Commun. - Green ICT, TIWDC 2013*, 2013, doi: 10.1109/TIWDC.2013.6664200.
- [26] I. Salah, M. M. Mabrook, K. H. Rahoma, and A. I. Hussein, “Throughput, Spectral, and Energy Efficiency of 5G Massive MIMO Applications Using Different Linear Precoding Schemes,” *Int. J. Electron. Telecommun.*, vol. 69, no. 1, pp. 189–194, 2023, doi: 10.24425/ijet.2023.144349.

- [27] B. Li, Y. Dai, Z. Dong, E. Panayirci, H. Jiang, and H. Jiang, “Energy-Efficient Resources Allocation with Millimeter-Wave Massive MIMO in Ultra Dense HetNets by SWIPT and CoMP,” *IEEE Trans. Wirel. Commun.*, vol. 20, no. 7, pp. 4435–4451, 2021, doi: 10.1109/TWC.2021.3058776.
- [28] S. Engineering, “Valentin Poirot ENERGY EFFICIENT MULTI-CONNECTIVITY FOR ULTRA-DENSE,” 2017.
- [29] G. Mao, *5G green mobile communication networks*, vol. 14, no. 2. 2017. doi: 10.1109/cc.2017.7868166.
- [30] F. Bahlke and M. Pesavento, “Energy Consumption Optimization in Mobile Communication Networks,” pp. 1–23, 2018, [Online]. Available: <http://arxiv.org/abs/1807.02651>
- [31] R. Chataut and R. Akl, “Massive MIMO systems for 5G and beyond networks—overview, recent trends, challenges, and future research direction,” *Sensors (Switzerland)*, vol. 20, no. 10, pp. 1–35, 2020, doi: 10.3390/s20102753.
- [32] A. Ghazanfari, *Power Control for Multi-Cell Massive MIMO*. 1852.
- [33] K. N. R. S. V. Prasad, E. Hossain, and V. K. Bhargava, “Energy Efficiency in Massive MIMO-Based 5G Networks: Opportunities and Challenges,” *IEEE Wirel. Commun.*, vol. 24, no. 3, pp. 86–94, 2017, doi: 10.1109/MWC.2016.1500374WC.
- [34] E. Björnson, L. Sanguinetti, J. Hoydis, and M. Debbah, “Designing multi-user MIMO for energy efficiency: When is massive MIMO the answer?,” *IEEE Wirel. Commun. Netw. Conf. WCNC*, pp. 242–247, 2016, doi: 10.1109/WCNC.2014.6951974.
- [35] E. Björnson, L. Sanguinetti, H. Wymeersch, J. Hoydis, and T. L. Marzetta, “Massive MIMO is a reality-What is next?: Five promising research directions for antenna arrays,” *Digit. Signal Process. A Rev. J.*, vol. 94, pp. 3–20, 2019, doi: 10.1016/j.dsp.2019.06.007.
- [36] S. Reddy Nalapatla Sreedhar Reddy Mamidala, N. Shashank Reddy, M. Sreedhar Reddy, P. Adrian Popescu, and P. Arlos, “Literature review on Energy Efficiency of Base Stations and Improving Energy Efficiency of a network through Cognitive Radio,” *Blekinge Inst. Technol.*, no. September, pp. 1–63, 2012.
- [37] R. M. Asif, J. Arshad, M. Shakir, S. M. Noman, and A. U. Rehman, “Energy Efficiency Augmentation in Massive MIMO Systems through Linear Precoding Schemes and Power Consumption Modeling,” *Wirel. Commun. Mob. Comput.*, vol. 2020, 2020, doi: 10.1155/2020/8839088.
- [38] V. Khodamoradi *et al.*, “Optimal energy efficiency based power adaptation for downlink multi-cell massive mimo systems,” *IEEE Access*, vol. 8, pp. 203237–203251, 2020, doi: 10.1109/ACCESS.2020.3037530.
- [39] A. Salh, N. S. M. Shah, L. Audah, Q. Abdullah, W. A. Jabbar, and M. Mohamad, “Energy-Efficient Power Allocation and Joint User Association in Multiuser-Downlink Massive MIMO System,” *IEEE Access*, vol. 8, pp. 1314–1326, 2020, doi: 10.1109/ACCESS.2019.2958640.

- [40] E. G. Larsson, O. Edfors, F. Tufvesson, and T. L. Marzetta, “Massive MIMO for next generation wireless systems,” *IEEE Commun. Mag.*, vol. 52, no. 2, pp. 186–195, 2014, doi: 10.1109/MCOM.2014.6736761.
- [41] M. Matthaiou, H. Q. Ngo, P. J. Smith, H. Tataria, and S. Jin, “Massive MIMO with a Generalized Channel Model: Fundamental Aspects,” *IEEE Work. Signal Process. Adv. Wirel. Commun. SPAWC*, vol. 2019-July, no. 1, pp. 1–5, 2019, doi: 10.1109/SPAWC.2019.8815518.
- [42] E. Björnson, L. Sanguinetti, J. Hoydis, and M. Debbah, “Optimal design of energy-efficient multi-user MIMO systems: Is massive MIMO the answer?,” *IEEE Trans. Wirel. Commun.*, vol. 14, no. 6, pp. 3059–3075, 2015, doi: 10.1109/TWC.2015.2400437.
- [43] H. Q. Ngo, E. G. Larsson, and T. L. Marzetta, “Energy and spectral efficiency of very large multiuser MIMO systems,” *IEEE Trans. Commun.*, vol. 61, no. 4, pp. 1436–1449, 2013, doi: 10.1109/TCOMM.2013.020413.110848.
- [44] H. Q. Ngo, *Massive MIMO: Fundamentals and System Designs*, no. 1642. 2015. doi: 10.3384/lic.diva-112780.
- [45] I. Salah, M. M. Mabrook, K. H. Rahouma, and A. I. Hussein, “Energy efficiency optimization in adaptive massive MIMO networks for 5G applications using genetic algorithm,” *Opt. Quantum Electron.*, vol. 54, no. 2, pp. 1–11, 2022, doi: 10.1007/s11082-021-03507-5.
- [46] M. Mimo and D. Systems, “ symmetry Energy Efficiency Optimization Based on Power Allocation in,” pp. 1–16, 2022.